1986-12

Sputtering of chemisorbed nitrogen from the (100)--planes of tungsten and molybdenum: a comparison of computer simulation and experimental results.

Mattson, Philip Jay

NAVAL POSTGRADUATE SCHOOL
Monterey, California

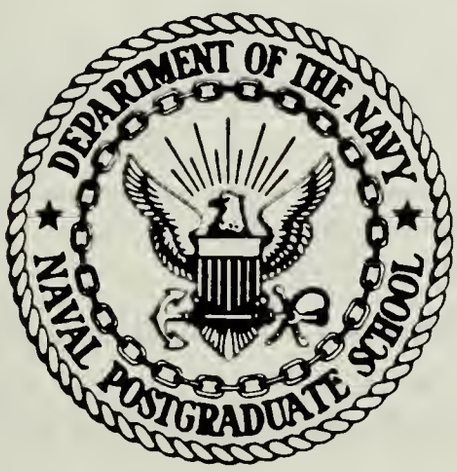

THESIS

SPUTTERING OF CHEMISORBED NITROGEN FROM THE (100) PLANES OF TUNGSTEN AND MOLYBDENUM: A COMPARISON OF COMPUTER SIMULATION AND EXPERIMENTAL RESULTS

by

Philip Jay Mattson

December 1986

Thesis Advisor: Don E. Harrison, Jr.

REPORT DOCUMENTATION PAGE

1a REPORT SECURITY CLASSIFICATION Unclassified	1b RESTRICTIVE MARKINGS
2a SECURITY CLASSIFICATION AUTHORITY	3 DISTRIBUTION / AVAILABILITY OF REPORT Approved for public release; distribution is unlimited
2b DECLASSIFICATION / DOWNGRADING SCHEDULE	
4 PERFORMING ORGANIZATION REPORT NUMBER(S)	5 MONITORING ORGANIZATION REPORT NUMBER(S)
6a NAME OF PERFORMING ORGANIZATION Naval Postgraduate School 6b OFFICE SYMBOL (If applicable) Code 61	7a NAME OF MONITORING ORGANIZATION Naval Postgraduate School
6c ADDRESS (City, State, and ZIP Code) Monterey, California 93943-5000	7b ADDRESS (City, State, and ZIP Code) Monterey, California 93943-5000
8a NAME OF FUNDING / SPONSORING ORGANIZATION 8b OFFICE SYMBOL (If applicable)	9 PROCUREMENT INSTRUMENT IDENTIFICATION NUMBER
8c ADDRESS (City, State, and ZIP Code)	10 SOURCE OF FUNDING NUMBERS PROGRAM ELEMENT NO / PROJECT NO / TASK NO / WORK UNIT ACCESSION NO

11 TITLE (Include Security Classification)
SPUTTERING OF CHEMISORBED NITROGEN FROM THE (100) PLANES OF TUNGSTEN AND MOLYBDENUM: A COMPARISON OF COMPUTER SIMULATION AND EXPERIMENTAL RESULTS

12 PERSONAL AUTHOR(S)
Mattson, Philip J.

13a TYPE OF REPORT	13b TIME COVERED	14 DATE OF REPORT (Year, Month, Day)	15 PAGE COUNT
Master's Thesis	FROM _____ TO _____	1986 December	86

16 SUPPLEMENTARY NOTATION

17 COSATI CODES			18 SUBJECT TERMS (Continue on reverse if necessary and identify by block number)
FIELD	GROUP	SUB-GROUP	Sputtering Computer Simulation Chemically Reacted Surfaces

19 ABSTRACT (Continue on reverse if necessary and identify by block number)

The Naval Postgraduate School simulation model, QDYN86, was used to examine sputtering of nitrogen from the (100) faces of single crystals of molybdenum and tungsten. The nitrogen placement was varied, and analyses were conducted on the sputtering cross sections of the nitrogen. The cases where the adatom was directly hit by the incident ion, or if it was sputtered due to the collision cascade process, were analyzed separately. The simulations were conducted to compare the results with Winter's recent work, and to build upon the efforts of earlier studies completed at the Naval Postgraduate School. It was found that placement of nitrogen at 0.245 A from the surface of molybdenum resulted in cross sections similar to those found by Winters. The effect of the mass of the substrate was verified, in that a substrate of greater mass results in a higher sputtering cross section. This agreed with Winters' findings, and conflicted with earlier conclusions of past theses. The adatoms apparently reduce the momentum available to create collision cascades, reducing the sputter yield ratio of the substrate when the ions directly hit the adatoms.

20 DISTRIBUTION / AVAILABILITY OF ABSTRACT	21 ABSTRACT SECURITY CLASSIFICATION
☒ UNCLASSIFIED/UNLIMITED ☐ SAME AS RPT ☐ DTIC USERS	UNCLASSIFIED

22a NAME OF RESPONSIBLE INDIVIDUAL	22b TELEPHONE (Include Area Code)	22c OFFICE SYMBOL
Don E. Harrison, Jr.	(408) 646-2877	Code 61Hx

DD FORM 1473, 84 MAR 83 APR edition may be used until exhausted
All other editions are obsolete

Approved for public release; distribution is unlimited

Sputtering of Chemisorbed Nitrogen from the (100) Planes of Tungsten and Molybdenum: A Comparison of Computer Simulation and Experimental Results

by

Philip Jay Mattson
Captain, United States Army
B.S., Oregon State University, 1977

submitted in partial fulfillment of the
requirements for the degree of

MASTER OF SCIENCE IN PHYSICS

from the

NAVAL POSTGRADUATE SCHOOL
DECEMBER 1986

ABSTRACT

The Naval Postgraduate School simulation model, QDYN86, was used to examine sputtering of nitrogen from the (100) faces of single crystals of molybdenum and tungsten. The nitrogen placement was varied, and analyses were conducted on the sputtering cross sections of the nitrogen. The cases where the adatom was directly hit by the incident ion, or if it was sputtered due to the collision cascade process, were analyzed separately. The simulations were conducted to compare the results with Winters' recent work, and to build upon the efforts of earlier studies completed at the Naval Postgraduate School. It was found that placement of nitrogen at 0.245 A from the surface of molybdenum resulted in cross sections similar to those found by Winters. The effect of the mass of the substrate was verified, in that a substrate of greater mass results in a higher sputtering cross section. This agreed with Winters' findings, and conflicted with earlier conclusions of past theses. The adatoms apparently reduce the momentum available to create collision cascades, reducing the sputter yield ratio of the substrate when the ions directly hit the adatoms.

TABLE OF CONTENTS

ACKNOWLEDGEMENT

I wish to thank those who preceded me, Steve Webb and Dirk Meyerhoff, and to acknowledge the fact that I drew quite heavily upon their efforts. I also wish to thank Professor Harrison for his patience, and the concern he showed throughout this exercise. Special thanks to my wife, Lyn, and my sons Karl and Curtis who put up with a lot during the final weeks of this project. Finally, special heartfelt thanks to Dana Majors, who's contribution to the effort could not go unrecognized.

I. BACKGROUND

A. HISTORICAL OVERVIEW

When a surface is bombarded by a beam of energetic particles under proper conditions, surface damage effects can be observed. This damage can manifest itself a number of different ways; as surface damage in the form of pits, blisters, and cones, and in the ejection of atoms from the target. This ejection of atoms during bombardment is called sputtering.

Sputtering was first discovered in 1853 by Grove [Ref. 1] when he observed the disintegration of the cathodes in glow-discharge tubes. He noted that the cathode material was deposited on the glass walls of the tubes. He called this process cathode sputtering. This erosion of the cathode was also noted by Plücker [Refs. 2-4]. Gassiot [Ref. 5] and Faraday also reported similar observations.

Fifty years passed before any explanation for these phenomena was proposed. In 1902 Goldstein [Ref. 6] presented evidence that the sputtering effects reported by Grove and Faraday were caused by positive atoms of the discharge impacting on the metal cathode of the tubes. Seven years later, in 1909, Stark proposed two models in an attempt to explain sputtering. The "hot spot model" considered the sputtered atoms to be the result of evaporation of target material from a small surface region due to localized heating by the ion beam. The "collision model" proposed that sputtering events were the result of a series of binary collisions initiated by a single ion [Ref. 7]. These models served to explain the experimental results at the time.

Later, in 1921, Thompson [Ref. 8] contributed to the field by suggesting that the atomic ejection was caused by the release of radiation as the ion struck the target. In the following years, a considerable amount of theoretical and experimental work was done. Bush and Smith [Ref. 9] in 1922 attempted to describe the ejection of atoms as the results of the expansion of gas adsorbed by the target material. The following year, Kingdon and Langmuir [Refs. 10, 11] conducted an experiment that suggested a momentum transfer ejection mechanism for sputtering. They bombarded thoriated tungsten with ions in a glow discharge tube. This was a special case of sputtering, where the thin surface film of thorium sputtered rather than the tungsten substrate.

In 1926, von Hipple and Blechschmidt [Refs. 12-15] proposed a theory that described sputtering as an evaporation of the surface atoms. Through spectroscopic techniques, von Hipple found that some of the sputtered atoms were in an excited state. He made further refinements on Stark's hot spot model, and made the first attempt to formulate a sputtering theory on the basis of local heating.

Lamar and Compton [Ref. 16], in 1934, published "A Special Theory of Cathode Sputtering," which led to the "thermal spike" concept. They suggested that binary collision processes were dominant in light-ion sputtering, where local evaporation predominates for heavy-ion sputtering. The thermal spike concept was based on momentum transfer between the bombarding ion and the lattice atoms. The theory suggested that a long lived high temperature volume persisted in the target after the collision cascade was completed.

One of the major problems facing experimentalists was the lack of ability to reproduce results. Penning and Moubis in 1940 published the results of their studies of the effect of pressure on sputtering yield [Ref. 17], (the sputtering yield is defined as the ratio of "sputtered" target atoms per incident ion). They found that the sputtering yield was reduced with an increase in pressure. Collisions between the ejected atoms and the surrounding gases at the higher pressures resulted in the backscattering of ejected atoms back onto the target surface, reducing the sputtering yield. When the background pressure was kept below 10^{-5} Torr, they were able to obtain reproducible results for ion energies in excess of 500 eV.

Keywell made an attempt to formulate Stark's collision model in terms of a neutron transport model originally developed for nuclear work [Ref. 18]. Wehner [Refs. 19 - 21], one of the major contributors to the modern understanding of sputtering, began publishing his findings in 1954. He discounted the evaporation model, and presented strong evidence for a momentum transfer process. He demonstrated the effects of crystal structure on the yield, and it became apparent that local heating alone could not account for the effects of sputtering. His observations revived interest in collision theory. One of his major contributions was the discovery of the anisotropic ejection patterns from monocrystalline targets, the now well known "Wehner spot pattern."

In 1956 Harrison [Ref. 22] applied statistical methods to sputtering. He developed a theory involving the interaction of two distribution functions; one for the crystal lattice and one for the ion beam.

He utilized transport theory and introduced the idea of ideal collision cross sections to explain sputtering from amorphous materials.

Sputtering, to this point, had been regarded as an annoying manifestation, one that eroded cathodes and filaments, contaminated plasmas, and was a general nuisance. There was great difficulty in obtaining reproducible experimental results. The theories proposed had not completely described the phenomena, and indeed have not yet today. Before continuing with the discussion of the current trends in sputtering theory and experimentation, a brief discussion of the currently "accepted" concepts of sputtering is in order.

B. PHYSICAL UNDERSTANDING

Sputtering is the ejection of atoms from a target when bombarded by energetic ion projectiles. The incoming ion collides with atoms in the bulk of the target material, transferring part of its kinetic energy and momentum to the target atoms. If the energy transferred to an atom is greater that the binding energy at the lattice site, then a primary recoil atom is created. This recoil atom may then collide with other atoms in the lattice, creating a collision cascade, transferring energy throughout the material. A surface atom may be ejected (sputtered) if the normal component of the energy transferred to it is greater than the surface binding energy of the lattice [Ref. 23]. Figure 1 illustrates three concepts of the sputtering process. Figure 1 (a) shows the interaction of the incident ion beam with the surface layer of the target. Figure 1 (b) illustrates the concept of the "thermal spike," where a high local temperature results in the evaporation of surface atoms.

Finally, Figure 1 (c) illustrates the collision cascade process, which is the current conceptual model for sputtering [Ref. 24].

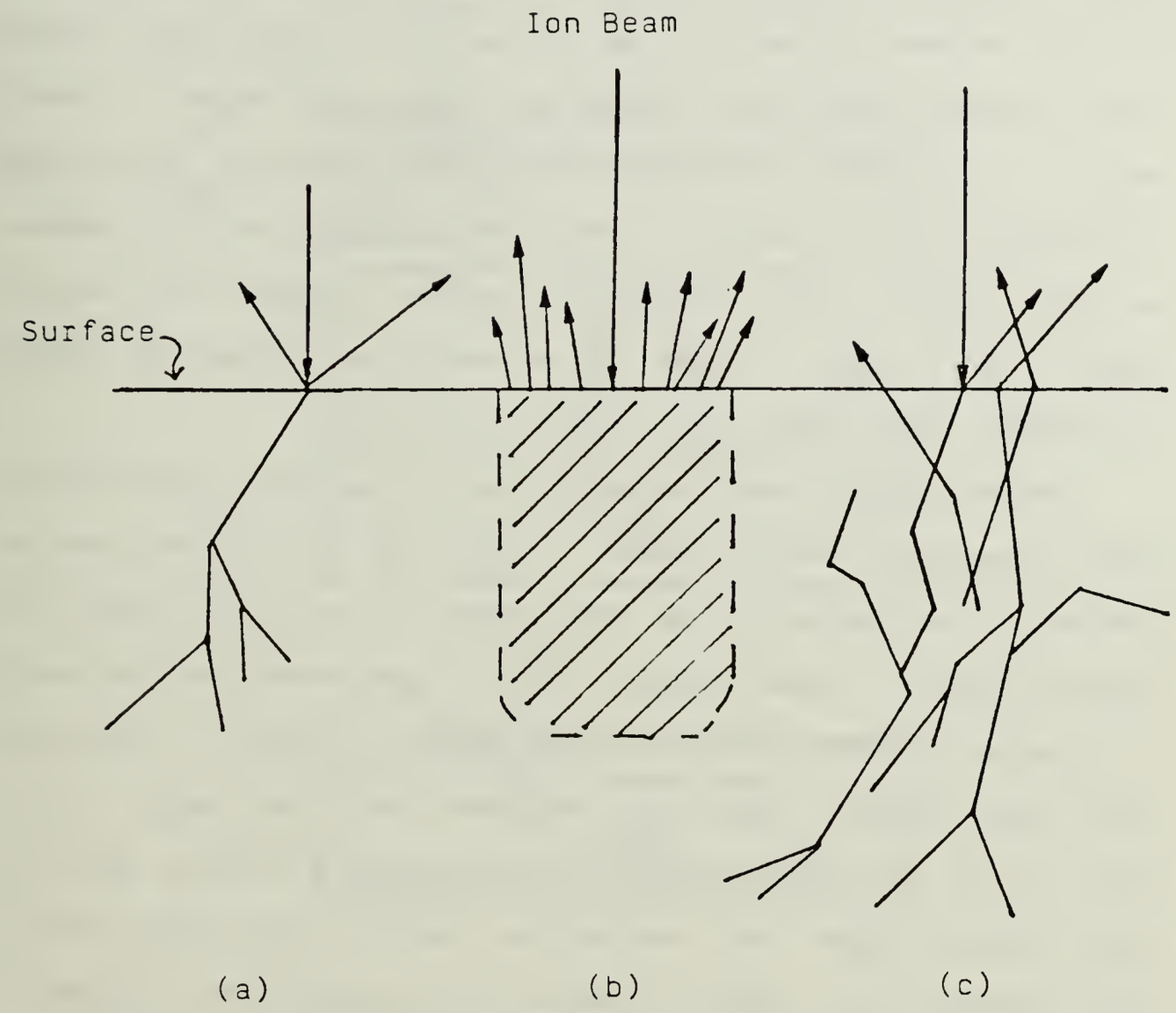

(a) Sputtering of surface atoms as a result of the interaction of the incident ion beam and the target surface.
(b) Surface atoms evaporated as a result of a thermal spike.
(c) Sputtering from a collision cascade, where energy is directed toward the surface from multiple binary collisions. [Ref. 24]

Figure 1. Models of the Sputtering Process.

The mechanisms for the sputtering of multicomponent materials (targets consisting of more than one atomic component) are more complicated. One of the simpler cases is the situation where a thin layer of a third component is placed on the surface of the thick target material. This is similar to the case examined by Kingdon and Langmuir in Reference 11. In this case, the added atoms on the surface are called adatoms and the bulk of the material is called the substrate [Ref. 25]. Examples of this situation were covered by Garrison, Winograd, and Harrison [Ref. 26] for oxygen on copper, and by Winters and Sigmund for nitrogen on tungsten [Ref. 27].

Winters proposed three mechanisms for the sputtering of the surface atoms, illustrated below in Figure 2. Layer (3) is the thin layer of adatoms on the surface of the thick target (2). An ion (1) bombards the target surface. In Figure 2(a), the ion hits the adatom, and the adatom is reflected off the substrate, either directly, or after it penetrates the target slightly. Figure 2(b) illustrates the case where the ion does not hit the adatom directly, but penetrates the target, and is in turn reflected itself. The reflected ion then hits the adatom, which is then sputtered off. Figure 2(c) shows the case where the ion causes an outward collision cascade, much like that illustrated in Figure 1(c). The outward flux of sputtered substrate in turn sputters the adatom.

The basic processes associated with sputtering are similar to those causing radiation damage in the bulk of a solid. Sputtering, however, usually involves atoms in the distorted surface layers (selvage) of the target material. The term, "selvage," is derived from the term "selvedge," which is a narrow band woven such that the edge will not

unravel. This analogy was extended to the distorted layers of the substrate material at its surface [Ref. 28].

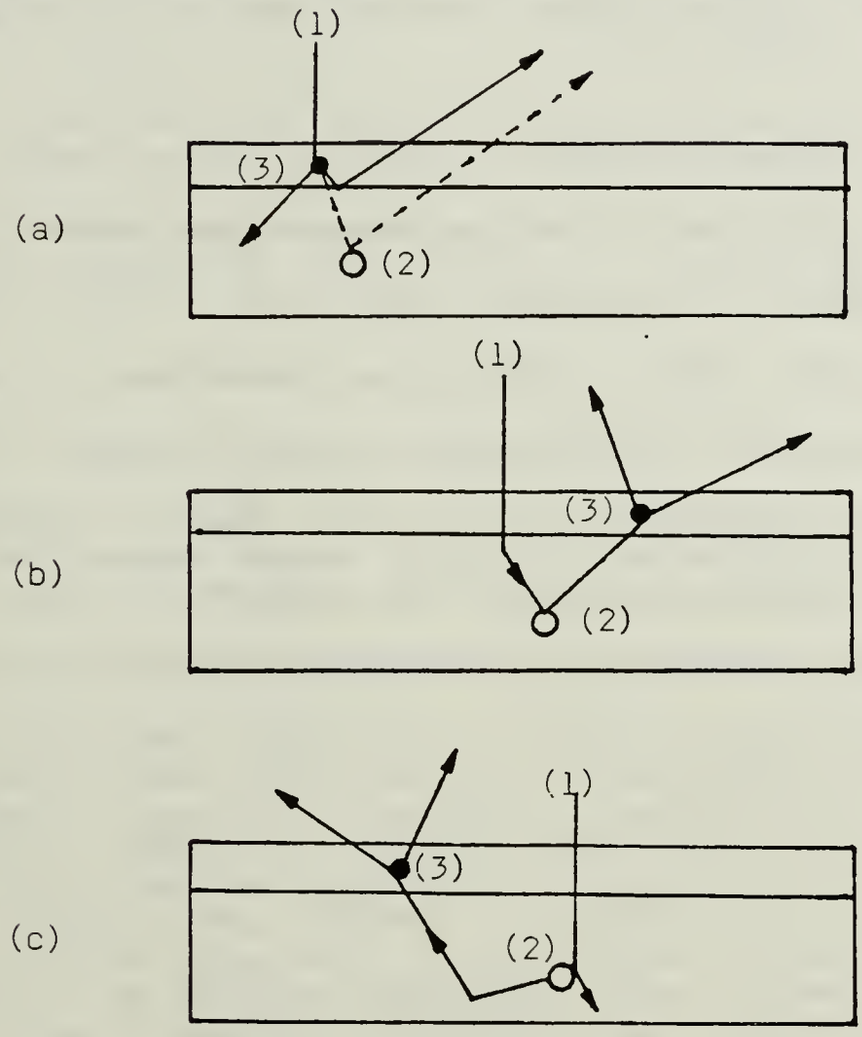

Figure 2. Three Proposed Mechanisms for the Sputtering of a Thin Layer on a Thick Target [Ref. 27].

Sputtering events take place in conditions far from thermal equilibrium, and are not evaporation of the material. Several factors can influence the sputtering yield, including incident ion energy, angle of incidence, ion type, target material, target crystal orientation, the presence of adsorbed molecules on the surface of the target, ambient

pressure, and numerous other factors. In order to obtain reproducible experiments, the following conditions must be met [Ref. 29]:

1. The target surface must be clean, that is free of contaminants in the form of adsorbed gases, lubricants from the vacuum pump, cleaning solvents, etc.

2. The gas pressure must be such that the mean free path of ions and sputtered atoms is large.

3. The ion current density must be high and the background pressure low so that formation of surface layers is prevented during the experiment.

4. The ions must strike the target at a known angle.

5. The energy spread of the incident beam must be small.

6. The ionizing conditions in the ion source should be such as to minimize the production of multiply charged species; the ions must be uniformly charged and mass separated.

7. The lattice orientation of monocrystalline targets must be known.

The field of sputtering is rich with terms used to describe the various observed and theoretical aspects of sputtering. Specific terms will be introduced as necessary to describe certain events, but two terms do merit mention here. Transmission sputtering is the ejection of atoms from the rear of a thin target. This occurs when sufficient energy is transported throughout the target to allow atoms to overcome the potential energy binding it to the target, allowing it to escape. Back-sputtering is the more familiar form, where atoms are ejected from the surface of the target material. Two other terms widely used, especially when discussing the sputtering of multicomponent materials are physical sputtering and chemical sputtering. Physical sputtering involves a transfer of kinetic energy from the incident particle to the atoms in the target, and the subsequent ejection of the atoms. Back

sputtering and transmission sputtering are manifestations of physical sputtering. Chemical sputtering is the result of a chemical reaction induced by the bombarding particle, which produces an unstable chemical compound on the surface of the target [Ref. 30].

C. THEORETICAL AND EXPERIMENTAL DEVELOPMENTS (1960 TO PRESENT)

In 1962, Wehner and others [Ref. 31] published data on the sputtering yields of metals and semiconductors in the 100-600 eV range. Later in 1966, Wehner [Ref. 32], in a report for Litton Systems published detailed results covering years of low energy sputtering research.

Silsbee [Ref. 33], in an effort to account for the angular distribution of ejecta, the "Wehner spot patterns," proposed a focused collision model, which allowed the transport of momentum in crystals along preferred directions. Experimental results had indicated that the sputtering yield for single crystal targets were dependent upon the crystallographic orientation of the target and the incident ion beam. This seemed reasonable, considering the "holes" observed in crystal models of when viewed from different planes. Focusing can be seen to contribute to the development of collision cascades within the target, it could not explain the Wehner spot patterns.

Sigmund and Lehmann [Ref. 34] proposed an alternative model, based on Boltzman transport equations, requiring the target surface to have an ordered surface. In this model, an atom in the collision cascade would sputter if its kinetic energy component normal to the surface was

sufficient to overcome the surface potential barrier. Thompson [Ref. 35] proposed another model to account for the spot patterns, in which the surface attraction for the escaping atom causes a refraction of its velocity vector away from the normal, resulting in a distortion of the angular distribution of ejecta. The theories of Sigmund and Thompson predict the sputtering yields of amorphous or polycrystalline targets fairly well, but do not accurately reflect the experimental results from the ordered surfaces of single crystal targets.

Numerous theories have been proposed, but none succeeds in fully describe all aspects of sputtering phenomena. Harrison [Ref. 36] in a recent review, stated that there were currently no less than seven types of sputtering theories in the literature. The statistical theories of Thompson [Ref. 35] and Sigmund [Ref. 34] predict the yield relatively well, and provide information on the ejected atom energy distribution function, and ejected atom angular distribution for polycrystalline targets. Kelly [Ref. 37] classifies sputtering processes according to time scales.

During this time, computer simulations were used to study sputtering. The models and codes now in use have been evolving for the past 30 years. The next section will present some basic philosophy of computer simulations, with applications to sputtering research.

D. COMPUTER SIMULATIONS

In 1960 a new tool was added to the scientific arsenal, aimed at examining sputtering. Gibson, Goland, Milgram and Vineyard [Ref. 38] published a report of the first computer simulation examining radiation

damage in a material. They simulated metallic copper and studied radiation damage events at low and moderate energies, up to 400 eV. In the model, one atom was given an arbitrary kinetic energy and direction of motion, simulating its having been struck by an energetic particle. This was one of the first published accounts of a computer simulation to study such events.

The high operating speed of computers makes them the natural choice for processing the numerous calculations required in a numerical analysis. The use of a computer simulation frees one from the constraints of general theories, and allows one to examine the basic physics of the system, to see how theory and experiment interact. In the words of Harrison [Ref. 36, p. 4]:

> A simulation is not a theory: it is a mathematical tool which is used to test the fundamentals of a theory. The computer can model a system with a minimum set of physical assumptions. This inherent simplicity helps to elucidate complex problems like sputtering: Simulations develop ideas which can then be exploited by both experimentalists and theorists.

Computer simulations fall into two general categories: time-step models and event-store models. An event-store program moves from event to event, skipping the intervening time. It maintains a list of potential future events (hence the name "event-store"), and checks and updates the lists to determine which event happens next. This model works well when the model is well understood, and the events are well separated in time. A time-step program carries the model forward for a short period of time, computes everything that happens to the system in that time interval, updates, and then continues on. This program is most useful when several things happen simultaneously. The time-step

program tends to be shorter than the event store program, but it also runs slower.

The event-store model used in sputtering research is based on the binary collision approximation (BC) [Ref. 39]. The assumption made is that each particle only interacts with one other particle at a time, and this other particle is usually assumed to be stationary. These models are inherently linear calculations [Ref. 40].

The time-step model used in this investigation is based on simultaneous multiple interactions (MI). Newtons laws, usually expressed in Hamiltonian form, are numerically solved for many particles. The MI model used in this thesis, QDYN86, is the latest revision of the MI program developed and used at the Naval Postgraduate School, and Pennsylvania State University. QDYN86 is a full-lattice simulation, which models the dissipation of an incident ion's momentum in a single crystal target, using classical mechanics. This program can generate different surfaces of several crystal structures. Adatoms can be placed on the surface of the crystal to simulate reacted surfaces. Specific details of the simulation will be presented in a later section of this thesis.

As can be seen, a considerable effort has been expended to study the mechanisms of sputtering. There is a practical reason for the interest, beyond the lure of pure research.

E. APPLICATIONS

Sputtering was long regarded as an undesired and little-understood effect [Refs. 41, 42]. It destroyed cathodes and grids in gas discharge

tubes, and contaminated plasmas and the surrounding walls [Ref. 43]. There was great concern about damage to spacecraft and satellites from sputtering. Efforts to understand and reduce these effects provided major impetus to the study of sputtering.

However; sputtering, in the form of the controlled removal of surface atoms from a target, is becoming especially important in its own right. The ability to precisely control an ion beam, and to remove atoms from surfaces is a very important tool in research, and in the manufacture of miniature components.

Sputter ion sources can be used for cleaning of surfaces, by removing adsorbed surface molecules to a degree that is impossible to achieve chemically or mechanically. The atoms sputtered from a surface can be analyzed in a mass spectrometer, giving information about the surface composition. One of the more important commercial applications of sputtering is the deposition of thin films on a large variety of substrates, especially useful in the manufacture of microelectronics. Sputtering is used in micromachining and depth profiling of thin films [Ref. 23].

There are applications of erosionally modified surfaces in the fabrication of optical, magnetic and surface acoustical technologies. Areas include grating fabrication, magnetic bubble technology, ion polishing, and reactive ion-beam etching [Ref. 44]. Research is being conducted to examine possible biomedical applications of sputtering. These include surface modification of biomedical materials, using sputtering for pathological discrimination, and with applications to implants and prostheses [Ref. 45].

One of the first commercial applications of sputtering was the use of sputtering for the deposition of solid film lubricants [Ref. 46]. Sputtering had the advantage that it allowed for the deposition of a variety of materials, on a large variety of substrates. The sputtered films are very dense, and strongly adherent. These properties are particularly useful for corrosion resistance and lubrication.

The list of possible applications could continue. The ability to understand and control the surface characteristics of a material to the atomic level is a very powerful tool. The majority of the work, especially in regards to the applications, is the result of considerable experimental effort. If one could better understand the mechanisms underlying the observed manifestations, then experiments could be better designed, and applications could be more quickly realized. It is toward this end that this research is conducted.

II. OBJECTIVES

A. PREVIOUS EFFORTS

The interaction of nitrogen with the (100) plane of tungsten has been widely examined. It was considered to be a useful system on which to base the development of adsorption kinetic and dynamic models [Ref. 47]. Winters [Ref. 48], in 1982, published a paper comparing the sputtering of chemisorbed nitrogen from polycrystalline targets of molybdenum and tungsten. His experiments showed that the nitrogen sputtering yield tended to increase as the atomic weight of the target substrate increased.

This paper of Winters provided the basis for two Masters theses at the Naval Postgraduate School. In 1983, Meyerhoff [Ref. 49] used an earlier version of Harrison's computer simulation sputtering model to study sputtering from nitrogen reacted (100) surfaces of tungsten and molybdenum targets. His goal was to compare the simulation results with the experimental results recently published by Winters in Reference 48. Meyerhoff concentrated on the reported mass effects. He concluded that while there may be a mass relation, the distance of the adatom from the substrate had a much more profound effect on the sputtering yield.

In 1986, Webb [Ref. 50] sought to further examine the adatom placement problem. Webb again used (100) surfaces of monocrystalline tungsten and molybdenum reacted with nitrogen and bombarded with argon

ions. He narrowed the range of the placement of the adatoms, and his results indicated that the adatoms were positioned above the (100) surface of the target plane.

In all these cases, the nitrogen adatoms were assumed to be in the four-fold position, as shown below in Figure 3. Meyerhoff assumed the nitrogen atom was slightly above the surface of the target plane, in a position of equal distance from its five nearest neighbors. Webb examined the nitrogen sputtering yield with the nitrogen placed at three different heights for molybdenum and two heights for tungsten.

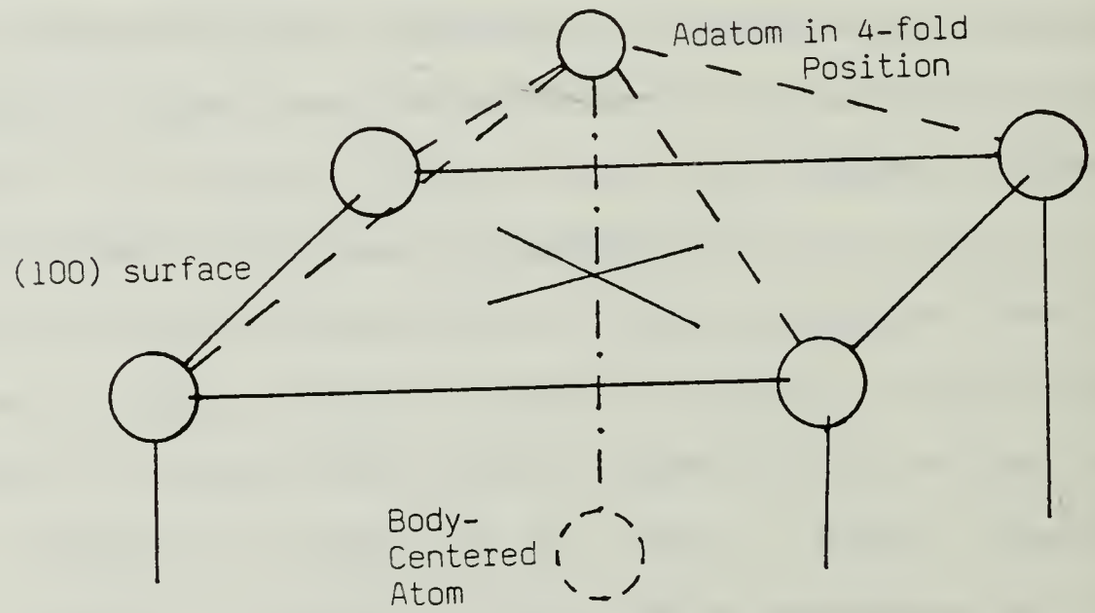

Figure 3. Nitrogen Adatom Placed in Four-fold Position in BCC Unit Cell.

The basis for the four-fold placement assumption is well established in the literature. An earlier work by Clavenna and Schmidt examined the interaction of N_2 with W(100) [Ref. 51]. They studied the binding states and condensation and desorption kinetics of nitrogen on W(100) using flash desorption spectrometry. They felt that the

nitrogen was in the four-fold position, but were uncertain exactly where the nitrogen was placed vertically in relation to the target surface. Adams and Germer [Refs. 52, 53] also examined the adsorption of nitrogen on tungsten. They used a combination of Low Energy Electron Diffraction (LEED), flash-desorption mass-spectrometry and contact potential measurements in their experiments. They refined their experiment by using the ^{15}N-isotope of nitrogen, in order to distinguish between nitrogen and CO present in the background gas. They felt that since the nitrogen atom was half the size of the tungsten atom, that it would sit in the well formed by the surface atoms of the substrate.

Griffiths, Kendon, King and Pendry [Ref. 54] examined target atom displacement due to the introduction of the nitrogen adatoms. They performed as series of LEED experiments with various nitrogen coverages and beam energies. They found that a fractional coverage of approximately 0.4 (defined as the ratio of the adatoms to the number of substrate atoms for a specific face of the target) was relatively stable. At higher coverages, of about 0.5, the nitrogen would be absorbed into the bulk at temperatures of about 1000 K. The 0.4 coverages were stable at this temperature. The model suggested by Griffiths, et. al. was a contracted domain structure, where the nitrogen occupies a four-fold hollow site, but that the four surface tungsten atoms are uniformly displaced towards the adatom. This leads to a series of "islands" consisting of 16 nitrogen atoms and the corresponding surface tungsten atoms, as shown in Figure 4. This type of formation was physically modeled by conducting a series of laser diffraction experiments. Laser diffraction gratings were constructed, with an average island

size of 4x4, and when illuminated by laser light produced diffraction patterns similar to those of the LEED beams on the actual target. Again, while this provided insight into the relative placement of the nitrogen on the surface, it did not provide any information on how the nitrogen was related vertically to the crystal surface.

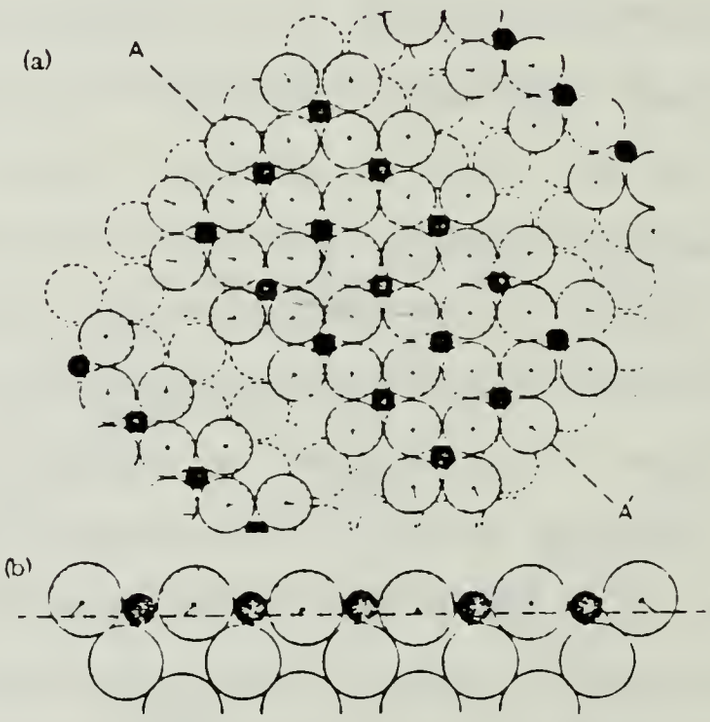

Illustrates contracted-domain structure of the 0.4 monolayer of Nitrogen on W(100) or Mo(100) surface. Large hatched circles illustrate the top layer of the substrate atoms, the small filled circles, the nitrogen atoms.

a) Plan view: Shows Domain and Boundary of Structure.

b) Cross Section through line AA. [Ref. 54, p.1586].

Figure 4. Suggested "Island" Formation of Nitrogen on Tungsten.

Meyerhoff assumed the equilbrium position of the nitrogen in his research. Webb examined equilibrium points both above and below the substrate surface plane. While there was a great body of information available on the adsorption of nitrogen on single crystal surfaces, there was little data on the sputtering of nitrogen from single crystal surfaces. This was rectified by a recent report by Winters [Ref. 55].

B. WINTERS' SINGLE CRYSTAL SPUTTERING EXPERIMENTS

This paper [Ref. 55] was a continuation of Winters' previous studies in the sputtering of chemisorbed nitrogen on tungsten. In his 1974 paper he proposed two mechanisms for the sputtering of nitrogen from the tungsten surface [Ref. 27]. He suggested that for low energy incident ions, the primary mechanism for the sputtering of the nitrogen was direct knock-on collisions with the impinging or reflected bombarding ions. The proposed mechanism for sputtering at higher bombarding energies included nitrogen atoms knocked away by sputtered substrate atoms. Winters' 1982 paper [Ref. 48] examined the sputtering of nitrogen from molybdenum and tungsten polycrystalline targets.

This latest report by Winters and Taglauer described experiments investigating the sputtering of chemisorbed nitrogen from W(100), W(111), W(110) and Mo(100) single crystal surfaces. The targets were bombarded with helium, argon and xenon ions in the energy range of 300 eV to 5000 eV. The relation between the sorbate mass, substrate mass and sputter yield were examined. Conclusions were drawn about thermal spikes, recoil implantation, and cascade mixing. Since these experiments were conducted on single crystal surfaces they provided some

basic information on the physics of the sputtering of multicomponent systems. Additionally, since the experimental data was derived from single crystals, they lend themselves more directly to computer modeling. A brief description of the experiment indicates how the system can be modeled in the computer simulation.

A Faraday cup and the four single crystal targets, W(100), W(111), W(110), and Mo(100) were mounted on a rotating manipulator. The targets were cleaned by heating to about 2500K for tungsten and 2200K for molybdenum by RF induction heating [Ref. 56]. The sample was exposed to $^{15}N_2$ until about 1/2 monolayer was adsorbed. This is in agreement with the findings of stable nitrogen adsorption on tungsten as mentioned in references 52 thru 54. The use of the ^{15}N isotope allowed one to isolate the adsorbed species involved in the study.

After the adsorption, an Auger spectrum was taken to ensure the absence of impurities from the sample surface. The ion beam was scanned by the Faraday cup in order to ensure beam uniformity, and to measure the beam current density. The ion beam was rastered across a 0.48 cm aperture, impinging at normal incidence upon the sample centered behind the aperture. A nitrogen Auger peak-to-peak intensity was determined as a function of the ion dose. Finally the sample, which was partially cleaned, was exposed to the ambient for approximately 600 sec after each run to monitor the readsorption of nitrogen. If readsorption was observed, the run was discarded.

The care taken in these experiments is quite apparent. The parameters of this experiment lend themselves quite well to computer simulation. Winters' also presented a comparison of the experimental

results with theoretical calculations based on the Sigmund-Winters theory for the sputtering of chemisorbed gas [Ref. 27]. One recommendation in the paper was :

> In particular, it would be useful to compare an extensive set of molecular dynamics calculations with both the experimental data and also the calculations presented in this paper. [Ref. 55, p. 26]

C. THESIS OBJECTIVES

The primary objective of this thesis is to examine sputtering from the (100) surfaces of single crystals of molybdenum and tungsten. Nitrogen will be placed in different equilibrium positions in relation to the substrate surface, and the system will be bombarded with argon ions of various energies at normal incidence. The effect of the mass of the substrate in relation to the sputtering yield will be examined.

III. COMPUTER SIMULATION AND MODEL DEVELOPMENT

A. THE COMPUTER MODEL AND RELATED PROGRAMS

1. QDYN86

The computer simulation used in this study is called QDYN86, which stands for the 1986 revision of the QDYN (Quick DYNamics) program used by Harrison at the Naval Postgraduate School. This program uses multiple-interaction (MI) logic in a time-step approach. The time-step logic is appropriate when many events occur simultaneously. The model is based on classical mechanics, using Newton's laws expressed in Hamiltonian form to simplify the calculations. The initial inputs to the program include the target crystalline structure, atomic masses and potential functions of the substrate, incident ion, and any adatoms; adatom locations, and bombarding ion angle of incidence, energy and impact point. The program develops the subsequent collision cascade, tracking the positions and velocities of the target atoms through time. The computations terminate when there is insufficient energy for any further ejections to occur.

The positions and velocities of the moving atoms are tracked through each time-step. In order to strike a compromise between excessive computer run time, and yet to maintain reasonable energy conservation, the time-step increment is variable. The time-step is determined by a specified distance divided by the highest atomic velocity in the

target. The distance chosen is 0.1 lattice units (LU), where the lattice unit is defined as one-half the lattice parameter, a_0 (for a cubic structure). The time-step increment is further modified by other factors which take into consideration the previous velocity, smoothing the transition in time.

The velocities and positions of every atom in the target are not calculated for each atom at every time-step. Again, this would consume excessive amounts of computer time. As a result, the forces are not computed on a specific target atom until the atom is struck by a moving atom. Atoms which rise above the target surface are put in a tentative list of ejected atoms. After further atom ejection from the target is unlikely, the atoms in this list are tested to see if they were travelling with sufficient velocity to overcome the attractive forces of the target atoms. Atoms which fail this test are added to the target, and are not counted as having been sputtered. Specific actions are taken for atoms that leave the bottom of the target, and through the sides. The program maintains, and periodically updates a listing of an atoms nearest neighbors. After the completion of a collision cascade, the program reinitializes, and prepares for another trajectory. A number of trajectories are run at different impact points in order to obtain better statistical results.

Subsequent sections in this chapter will provide further details on the choice of potential functions, substrate characteristics, impact points, and other factors as they pertain to this study. A number of other articles provide more detailed information on the QDYN simulation, and other molecular dynamics simulations. Reference 36

provides a good overview of sputtering models. Harrison and Jakas compared the MI and binary collision models [Ref. 57], and with Webb, examined a hybrid code between the two models [Ref. 58]. The most recent, and most detailed discussion of the QDYN program by Harrison and Jakas identified uses of the program for studies involving insulators and semiconductors [Ref. 59].

2. Ancillary Programs

A number of other programs are used to support the main simulation. These programs are identified and are briefly described below.

a. QDYNLIBB (QD86LIBB)

This program forms a library from which the main program derives routines for calculating the forces and potentials. The potential and forces tables are dimensioned to 10000, and support four potential functions. Adatom routines are available for placing adatoms on the surface of the target, or creating steps or vacancies.

b. TARGLIBB

This program forms a library of routines used for generating (100), (110), and (111) faces of BCC, FCC and Diamond lattice targets. A rotated FCC (001) lattice can also be generated.

c. ANMOL

This program analyzes the basic data set generated by the main program. The output of the main program consists mainly of a listing of the positions and velocities of the atoms. ANMOL uses this data file to calculate which atoms are sputtered, from which layer in the target lattice they originated, and rotational and vibrational analysis

of the ejected atoms. Determination of multimers, ejection time distributions and ejection energies are also calculated.

d. ANPLOT

This is a program used to interface with the DISSPLA graphics package. ANPLOT is used to generate graphical analyses of the data file generated by the main program.

e. POTTER

This program is used to generate potential functions. An abbreviated input deck is read by POTTER, and two data files are generated. These files, FORCE DATA and ENERGY DATA, are used by the next program to obtain a graphical representation of the functions.

f. POTPLOT

This is another graphics routine that interfaces with the DISSPLA graphics package. POTPLOT uses the data files generated by POTTER, and produces a liner plot of the potentials, and a semi-log plot of the forces. This allows one to quickly determine which modifications must be made to obtain the proper shaped curve for the desired potential and force function. The potential functions used in this thesis were generated using this program.

B. SUBSTRATE AND ADATOM PROPERTIES

The systems of nitrogen-on-molybdenum and nitrogen-on-tungsten were chosen by Winters for his sputtering experiments for a very specific reason. Many of the physical parameters of the two substrate materials are very similar, and the behavior of nitrogen with each was thought to be almost identical also. This provided a means of physically reducing

the variables in the system, enabling him to isolate and concentrate on the mass difference of the two materials. A summary of the key physical parameters for the two systems is show below in Table 1.

TABLE 1. PHYSICAL DATA FOR MOLYBDENUM AND TUNGSTEN.

	MOLYBDENUM	TUNGSTEN
Atomic Number (Z)	42	74
Atomic Weight (amu)	95.94	183.85
Atomic Radius (A)	1.363	1.371
Density (gm/cm^3)	10.22	19.3
Crystal Type	BCC	BCC
Lattice Constant (A)	3.147	3.165
Lattice Unit (1/2 a_o, A)	1.5735	1.5825
R_e (A)	2.8	2.894
Valence	+4	+4
Ionic Radius (A)	0.70	0.70
Cohesive Energy (eV)	6.82	8.90
Binding Energy of N (eV)	6.5	6.5

Data for Table 1 derived from References 60-62.

Table 1 illustrates the high degree of similarity between some of the physical properties of molybdenum and tungsten. Nitrogen is assumed to occupy the four-fold position on the surface of both materials. The major difference between the two materials is the significant difference in mass and Z. The pertinent physical properties of the adatom, nitrogen; and the incident ion, argon; are summarized below in Table 2.

TABLE 2. PHYSICAL DATA FOR NITROGEN AND ARGON.

	Nitrogen	Argon
Atomic Number (Z)	7	18
Atomic Weight (amu)	15	39.94

Data for Table 2 derived from Reference 63.

C. POTENTIAL FUNCTIONS

1. General

The dynamics of the atomic interactions are controlled by the choice of the potential functions used to describe the potential energies and forces felt by the atoms. There is no "right choice" for a potential function in these types of simulations, indeed, Harrison has called the development of useful potential functions for simulations a "black art". A number of different potential functions can and have been used in sputtering simulations. Harrison has found that the choice of potential function parameters do not overly affect the outcome of the simulation [Ref. 64]. The potential functions used in this investigation are described briefly below. Detailed discussions of these, and other potential functions can be found in Torrens [Ref. 65]. A number of survey articles by Harrison describe more fully how the potential functions are applied to the simulations [Refs. 36, 57-59].

a. Born-Mayer

The Born-Mayer potential function is a purely repulsive function. This function is used for intermediate atomic separations. The form of the function is

$$V(r) = a \exp(-br). \qquad (1)$$

b. Moliere

The Moliere potential function is another purely repulsive potential function, of a slightly different form. It is called a "Screened Coulomb Potential," and is an approximation of the Thomas-Fermi screening function. The general form of the potential is

$$V(r) = (Z_1 Z_2 e^2 / r)[0.35 \exp(-0.3r/a) + 0.55 \exp(-1.2r/a) + 0.1 \exp(-6.0 r/a)] . \quad (2)$$

The term "a" is called the "Firsov length" defined as follows:

$$a = K\ 0.8853\ a_b / (Z_1^{1/2} + Z_2^{1/2})^{2/3} . \quad (3)$$

The "a_b" term is the Bohr radius,

$$a_b = h^2 / 4\pi^2 me^2 = 0.5292\ A. \quad (4)$$

The "a" parameter may be modified, since the Moliere potential is an approximation to the Thomas-Fermi function. When K = 1, the potential is pure Moliere; when K is set unequal to 1 then the function is known as a "modified Moliere" potential function.

c. Morse

The Morse potential is both attractive and repulsive, depending upon the separation distance, "r". It has the form:

$$V(r) = D_e \exp[-2\alpha (r-r_e)] - 2D_e \exp[-\alpha(r-r_e)]. \quad (5)$$

The term, D_e is the well depth, and r_e is the equilibrium separation of an atomic pair, and alpha is a scale factor which controls the shape of

the potential well. The function is attractive for $r > r_e$, and repulsive for $r < r_e$.

d. Composite Morse-Moliere

The composite Morse-Moliere potential function is used to more closely model the dynamics of the sputtering events. The repulsive wall of the Morse potential is joined with a cubic spline to the Moliere potential, to form a single potential function which can be used over long ranges. The two functions are joined by varying the alpha term of the Morse, and the "a" term of the Moliere to obtain an intersection which has a smooth, continuous slope. The repulsive wall governs the collision dynamics, and the attractive well of the Moliere controls the sputtering by determining whether an atom will escape the surface of the target.

2. Selection of Potential Function Parameters

a. Substrate-Substrate, Adatom-Adatom Function Parameters

A composite Morse-Moliere function was used for the solid phase Mo-Mo and W-W potential functions. The specific parameters used in this thesis follow those developed by Webb, with one exception. The function used for the W-W forces had a discontinuity as shown in Figure 5. This was smoothed by changing the R_a value. The potential curves are shown in Figure 6.

The nitrogen-nitrogen potential function is a pure Morse potential function. The tabulated data for the solid phase W-W, Mo-Mo, and N-N potential functions is listed below in Table 3.

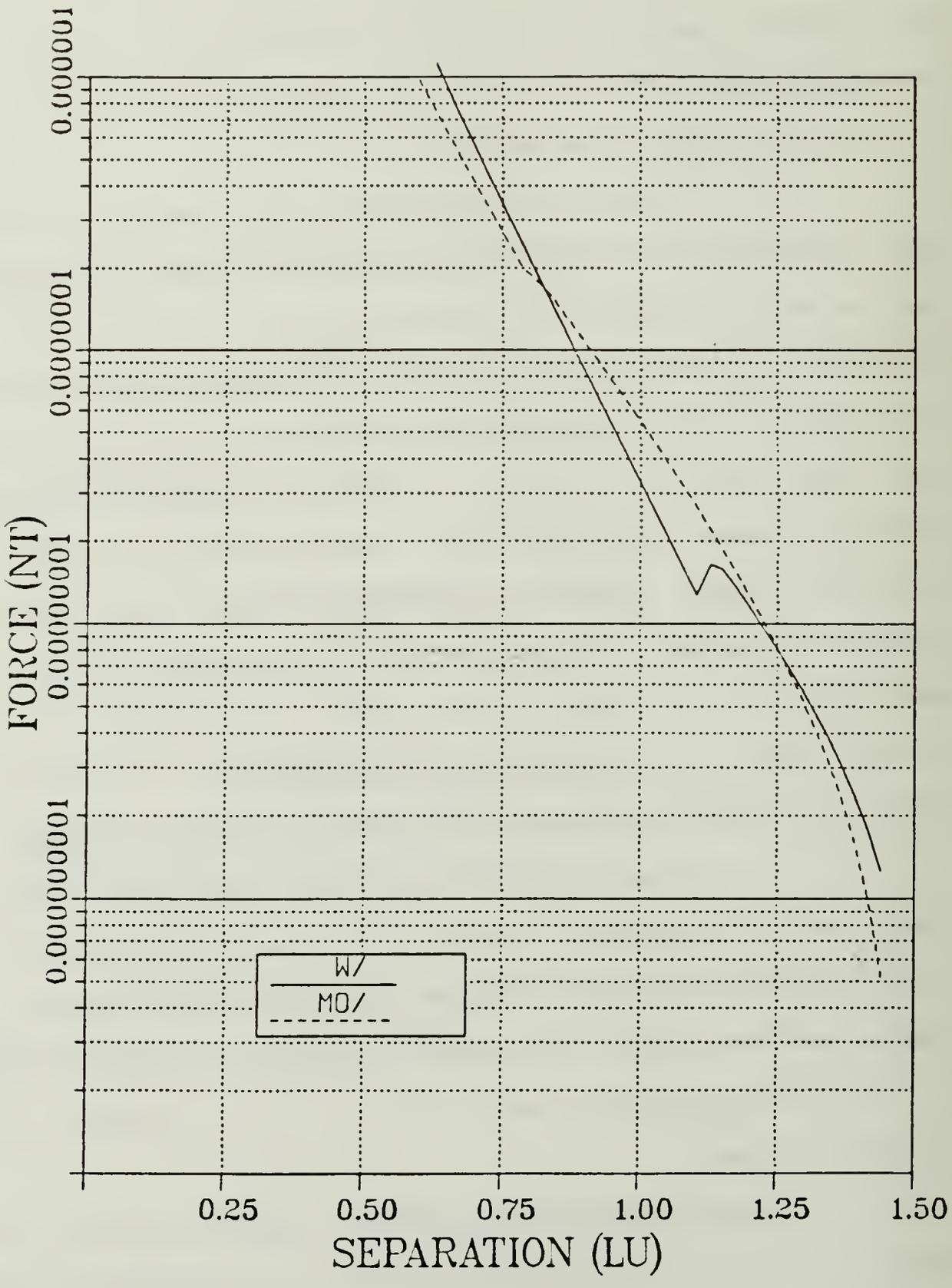

Figure 5. W-W and Mo-Mo Forces

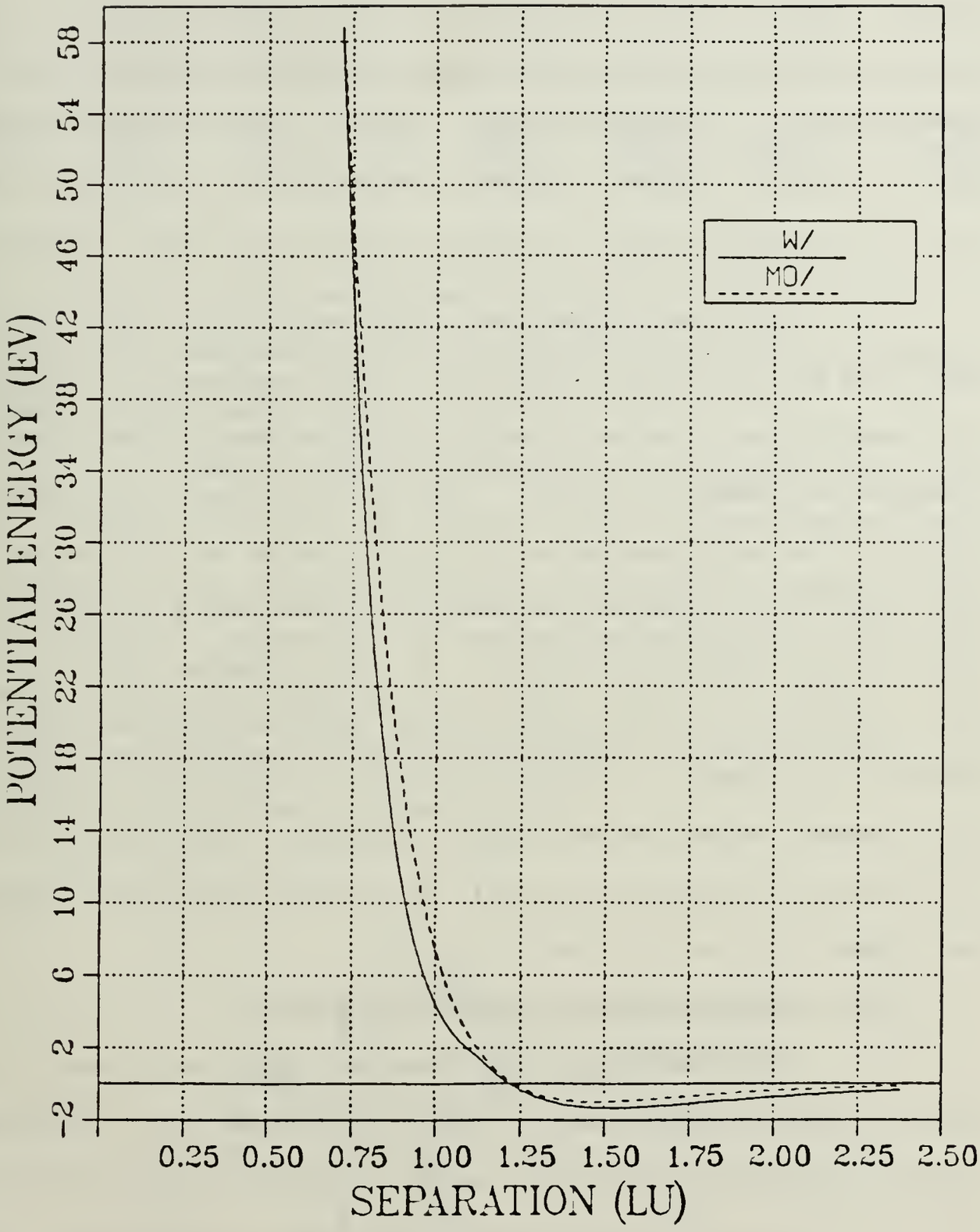

Figure 6. W-W and Mo-Mo Potentials Generated By Webb.

TABLE 3. SOLID PHASE POTENTIAL PARAMETERS

	D_e (eV)	R_e (A)	α (A^{-1})	k	R_a (LU)	R_b (LU)	R_c (LU)
Mo-Mo	0.997	2.800	1.519	0.0	0.790	0.830	2.40
W-W	1.335	2.894	1.200	0.0	0.80	1.130	2.40
N-N	7.373	1.098	2.700	0.0	0.0	0.0	1.71

The α and k terms were used to match the slopes of the Morse and Moliere potential functions, as mentioned earlier. The value of D_e was selected in order to obtain the proper cohesive energy for the substrate as shown in Table 1. The R_e term is the nearest neighbor distance. The spline boundaries, R_a and R_b, are in turn a function of the α and k values selected, and should be no more than ½ LU apart. This topic will be covered in more detail in the following section. The final value, R_c, is a distance over which the force and potential calculations are made, a cut-off distance. This allows for interactions only between nearest and next-nearest neighbors. This value is set at 1.71 LU for all interactions except the substrate-substrate interactions, where it is set at 2.40 LU.

b. MO-N, W-N Potential Function Parameters

Six new potential functions were generated to examine the effect of adatom placement on the sputtering cross section. The FORTRAN routines POTTER and POTPLOT were used to help generate these functions. The first step was to select an elevation to place the adatom, and from that to determine R_e, the nearest neighbor separation distance. R_e is the distance measured vertically between the cubic center and the adatom, as shown in Figure 7. These values were then input to POTTER.

POTTER generates two data files used by the POTLOT routine to plot the potential and forces curves. The R_a, R_b, k, and alpha values are modified so that a smooth curve is plotted for both the potentials and forces. Once this rough determination is completed, then D_e is modified and evaluated by running a single trajectory at one time-step under CMS in order to obtain the proper sublimation energies. D_e is modified so that the sublimation energy of the nitrogen to the substrate is maintained at 6.5 eV. The binding energy of the adatom is one-half the sublimation energy, or 3.25 eV.

After the sublimation energy has been properly set, then the revised values for D_e are once again run through POTTER and POTPLOT in order to insure that the curves have the necessary smooth slopes. These graphical methods for rapidly evaluating potential function parameters have greatly eased the process for generating potential functions. The values for the Mo-N and W-N potential functions used in this thesis are listed below in Tables 4 and 5.

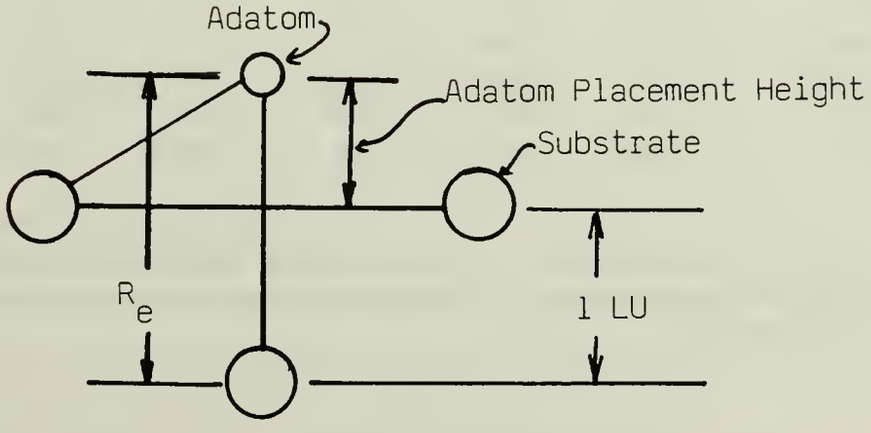

Figure 7. Physical Dimensions Used in Potential Function Calculations.

TABLE 4. Mo-N POTENTIAL FUNCTION PARAMETERS

Location (A)	D_e (eV)	R_e (A)	α $(A)^{-1}$	k	R_a (LU)	R_b (LU)	R_c (LU)	
-0.05	2.970	1.524	2.60	0.80	0.540	0.560	1.71	**
0.146	2.0428	1.720	2.20	0.80	0.540	0.560	1.71	
0.245	1.997	1.738	2.143	0.80	0.500	0.520	1.71	**
0.290	1.747	1.864	2.20	0.0	0.560	0.520	1.71	
0.335	1.672	1.908	2.20	0.0	0.520	0.560	1.71	
0.38	1.60	1.950	2.15	0.0	0.720	0.750	1.71	**

Note: Rows marked with ** indicate parameters developed by Webb, and used in both theses. Unmarked rows indicate new potential function parameters.

TABLE 5. W-N POTENTIAL FUNCTION PARAMETERS

Location (A)	D_e (eV)	R_e (A)	α $(A)^{-1}$	k	R_a (LU)	R_b (LU)	R_c (LU)	
-.05	3.292	1.524	2.85	0.8	0.65	0.67	1.71	**
0.1623	2.341	1.7448	2.75	0.0	0.75	0.80	1.71	
0.2464	2.013	1.8289	2.60	0.0	0.80	0.85	1.71	
0.325	1.774	1.9075	2.45	0.0	0.85	0.90	1.71	
0.487	1.712	1.960	2.32	0.9	0.83	0.85	1.71	**

Note: Rows marked with ** indicate parameters developed by Webb, and used in both theses. Unmarked rows indicate new potential function parameters.

c. Ion-Substrate, Ion-Adatom Functions. The potential function parameters for the incident ion must be considered. The target is bombarded by Argon ions, but for the purposes of these calculations, the charge on the ion is neglected. The ion is charged so that it can be accelerated to the desired energy to bombard the target. Since the incident ion is a noble gas, the event that it will react with the molybdenum, tungsten or nitrogen atoms other that through simple collision process is unlikely. The potential functions are correspondingly modified Moliere. The potential function parameters are listed below in Table 6.

TABLE 6. AR-N, AR-MO, AND AR-W POTENTIAL PARAMETERS

	D_e (eV)	R_e (A)	α $(A)^{-1}$	k	R_a (LU)	R_b (LU)	R_c (LU)
Ar-N	0.0	0.0	0.0	0.0	1.71	1.71	1.71
Ar-Mo	0.0	0.0	0.0	0.0	1.71	1.71	1.71
Ar-W	0.0	0.0	0.0	0.0	1.71	1.71	1.71

Figure 8 shows the Nitrogen-Nitrogen potential function, and Figure 9 shows the Ar-N, Ar-Mo, and Ar-W potential functions.

d. Vacuum Phase Potentials

Once atoms have sputtered from the surface of the target, there is a probability that further interactions can occur in the vacuum phase. Vacuum phase interactions were not emphasized in this study, but for the sake of completeness, the vacuum phase parameters derived in Webb's thesis are included in Table 7. There is little available data

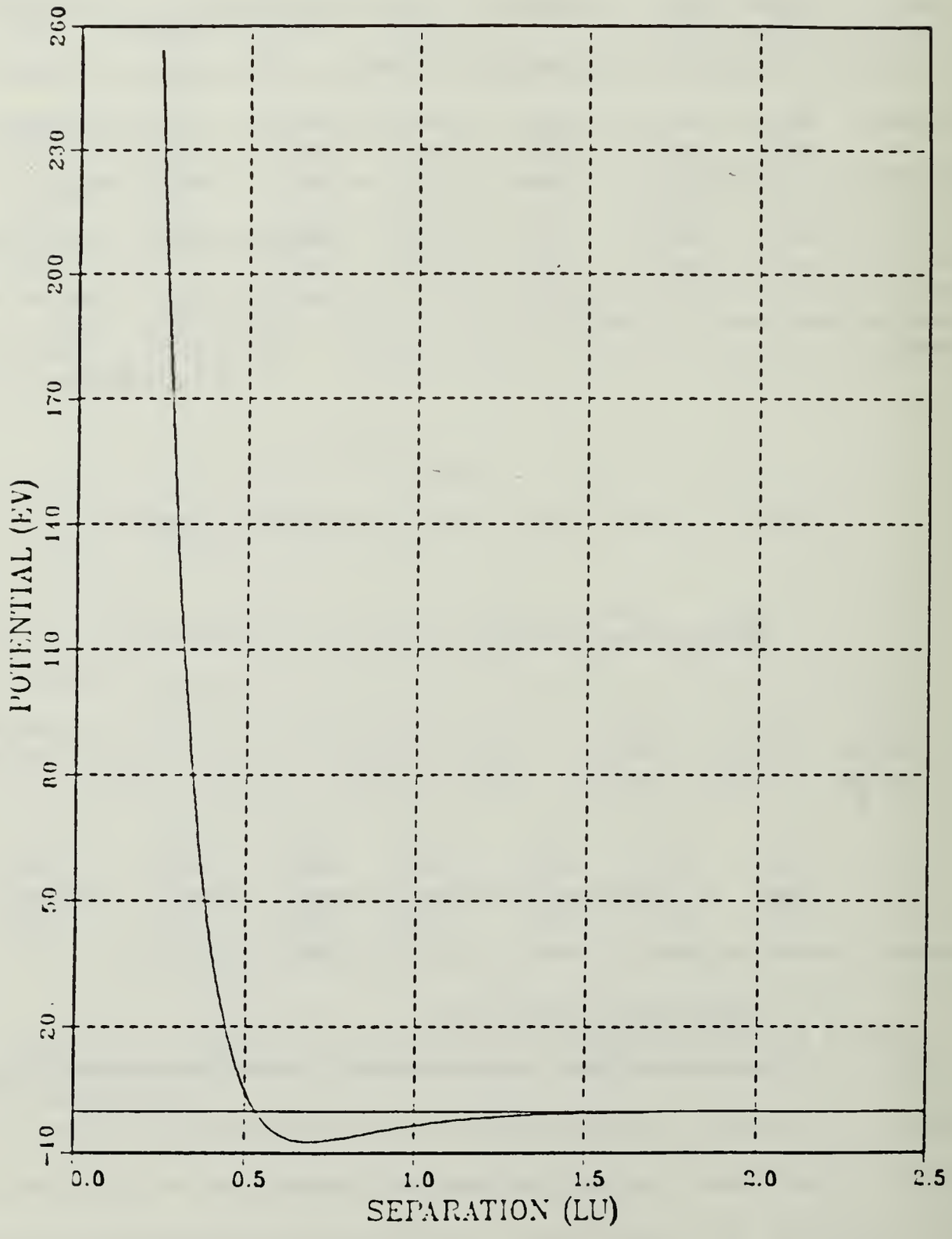

Figure 8. Nitrogen-Nitrogen Potential Function.

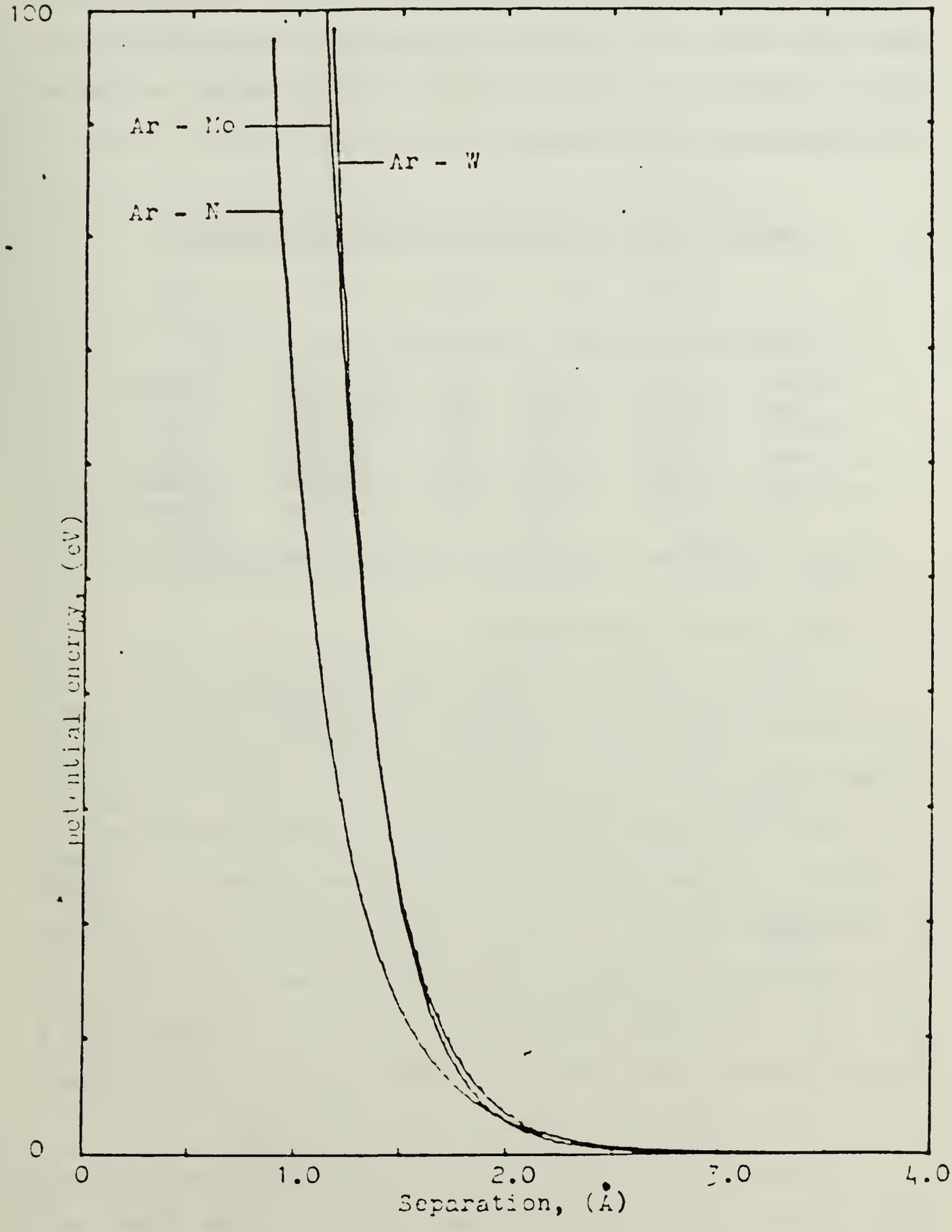

Figure 9. Ar-Mo, Ar-N, and AR-W Interatomic Potential Functions.

for the Mo-Mo, W-W, Mo-N, and W-N systems. The following substitutions were made, using similar systems to those examined in this study. The Ag-Br system was used fro Mo-Mo, and VO was used for Mo-N. Data on the N-N system was available and used. [Refs. 50, 65].

TABLE 7. VACUUM PHASE POTENTIAL FUNCTION PARAMETERS

	D_e (eV)	α $(A)^{-1}$	R_e (A)	Ω	Ωx	
Mo-Mo	1.700	1.790	2.390	247.000	0.679	
N-N	5.760	3.359	1.098	2358.570	14.320	
Mo-N	6.100	1.965	1.524	1020.000	4.700	
W-W	3.100	1.450	2.470	308.399	0.960	
W-N	4.900	2.159	1.738	967.000	4.850	
RHC	2.900	1.560	2.390	1050.000	5.000	**

Note: The Rhodium vacuum data was used in some cases.

D. TARGET and IMPACT AREA CONCERNS

One characteristic of MI simulations of this type, is that finite target sizes are used. Two concerns must be balanced in determining the optimum target size. First one must try to have a target of sufficient size such that the majority of the sputtering events are contained. If the target is too small, then information will be lost due to a failure of containment event. On the other hand, an excessively large target will require excessive computer time to complete each trajectory. In this thesis, two target sizes were used. At the 500 eV energy level, a 19x6x19 target was used, and at higher energy levels a 23x8x23 target size was used. Webb used the larger target in his thesis.

Nitrogen atoms were placed in the four-fold position on both target sizes. 40 atoms were placed on the smaller target, and 60 atoms were

placed on the larger. In both cases this resulted in a fractional coverage of approximately 0.4, which corresponds to the contracted domain structure of Reference 54. The nitrogen adatom coverage is shown in Figure 10, corresponding to the (001) face of the substrate material. Table 8 lists target area and nitrogen coverage parameters.

TABLE 8. TARGET AREA AND ADATOM COVERAGE PARAMETERS

Target Size	19 x 6 x 19		23 x 8 x 23	
Substrate	Mo	W	Mo	W
No. Nitrogen	40	40	60	60
Area (cm^2)	8.02×10^{-14}	8.11×10^{-14}	1.20×10^{-13}	1.21×10^{-13}
Fractional Coverage	0.4	0.4	0.42	0.42
Coverage (atoms/cm^2)	4.99×10^{14}	4.93×10^{14}	5.0×10^{14}	4.96×10^{14}

Another factor which impacts on the run time of the simulation, and the statistical accuracy of the results is the number of impact points, or trajectories run. The impact points are designated by a pre-selected "pin-point", and then the trajectories impact in a representative area based on this point. Two types of pin-points were used. In one, the "hit" case, a nitrogen adatom is placed in the representative area, and can be hit directly by the incoming ion. The other, "non-hit" case, does not have a nitrogen atom in the representative area. The simulations were run in this study with 150 trajectories per pin-point, or 300 trajectories per complete run. Previous studies used 300 trajectories per pin-point, for a total of 600 trajectories per case.

The pin-points for the "hit" case were located at (8.000, 6.000) for the 19x6x19 target lattice, and (13.000, 15.000) for the 23x8x23

target. The non-hit cases were run with pin-points at (8.000, 8.000) and (11.000, 11.000) respectively. These pin-points are measured on the x- and z- axes. The representative areas and pin-points are also shown in Figure 10.

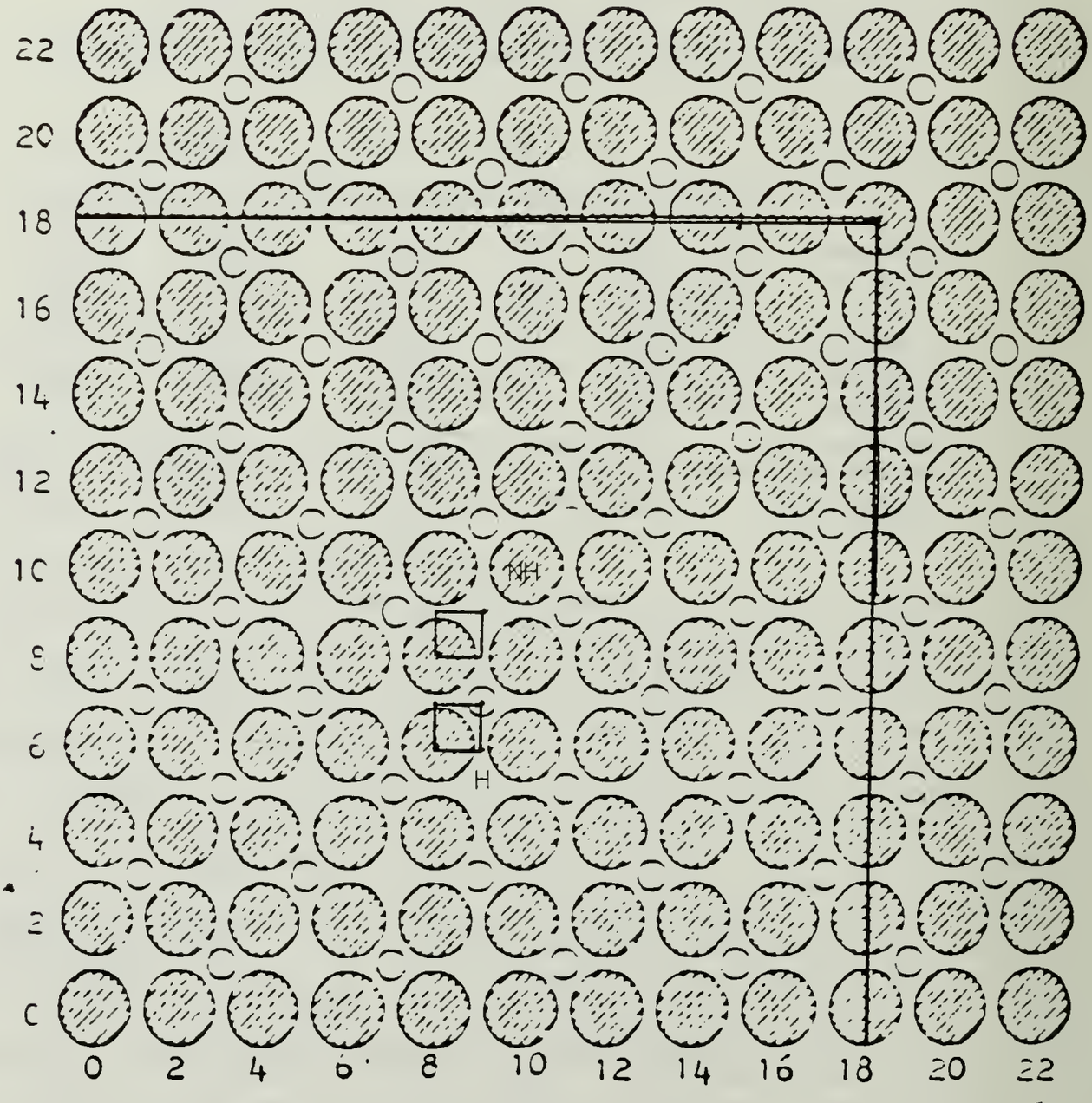

Small circles represent nitrogen atoms.
"H" indicates "Hit" representative area.
"NH" indicates non-hit representative area.

Figure 10. Top View of Nitrogen Reacted Surrace.

IV. RESULTS AND DISCUSSION

A. GENERAL

1. Sputtering Cross Sections

The concept of the sputtering cross section is key to the analyses in this study. The derivation of the cross section is carried out in detail in Appendix A. The basic methodology used by Winters was adapted to the simulation, and the following relation was derived:

$$\sigma_N = - \{\ln (1 - Y/N_0)\} A_0 \ . \qquad (6)$$

Y is the sputter yield from the simulation, σ_N is the Nitrogen sputtering cross section, N_0 is the initial number of adatoms placed on the target and A_0 is the surface area of the target.

2. Winters' Results

Winters' experiment involved the bombardment of the (100) plane of molybdenum and tungsten with argon, xenon and helium ions in energies from 300 eV to 5 keV. The cases studied in this thesis concerned argon ions of the 500 eV to 2 keV range on Mo(100) and W(100). Winters' presented results from his experiments, and theoretical calculations from the Sigmund-Winters theory of multicomponent sputtering. The results that fall within the bounds of this study are tabulated below in Table 9 [Ref. 55 p. 29].

TABLE 9. WINTERS' THEORETICAL AND EXPERIMENTAL CROSS SECTIONS AS A FUNCTION OF ION ENERGY

Ion Energy (eV)	Experiment (10^{-16} cm^2) Mo(100)	W(100)	Calculation (10^{-16} cm^2) Mo(100)	W(100)
500	5.6	8.6	6.0	6.9
1000	6.5	8.8	6.8	7.4
2000	6.8	9.0	8.0	8.1
3000	6.6	8.6	8.9	8.6

3. Previous Theses at the Naval Postgraduate School

a. Meyerhoff

Meyerhoff's thesis in 1983 examined clean and nitrogen reacted molybdenum and tungsten (001) surfaces bombarded with argon ions of energies ranging from 500 eV to 3 keV. Nitrogen was placed in the four-fold position, and was examined at two elevations above the (001) surfaces. The effect of the mass of the substrate was examined by replacing the Mo-mass with the tungsten mass. Meyerhoff concluded that the sputtering cross section of the nitrogen was more dependant upon the distance of the adatoms above the surface then upon the mass of the substrate. [Ref. 49]

b. Webb

Webb, in early 1986, continued the study of nitrogen on molybdenum and tungsten. He refined the potential functions used by Meyerhoff, and performed basic sputtering research using the QDYN simulation. He studied the sputtering cross section of nitrogen for placement at three different heights in relation to the (001) surfaces of

molybdenum and tungsten. He concluded that the nitrogen was most likely located above the surface, as opposed to being in the well formed by the surface atoms.

4. Analyses Conducted in This Study

The scope of the analyses conducted in this study differed somewhat from previous theses. The previous studies did not differentiate between the effects of the incident ion initially hitting the adsorbed nitrogen, or the substrate. The simulations were run with impact points covering both cases, but the results were not looked at separately. In this study, the two cases were analyzed separately. This was done in order to gain insight into possible sputtering mechanisms as outlined earlier.

The nitrogen sputtering cross sections were examined at 500 eV (low energy sputtering) and 2 keV (high energy sputtering). The hit and no-hit cases were examined in order to determine the sputtering mechanism of the nitrogen. The yield of the substrate was examined, and the ratio of the bare to the reacted substrate yields was used as a measure to determine the relative effects of the adsorbed nitrogen. The purpose of this analysis was to determine if the nitrogen enhanced the sputtering yield of the nitrogen, particularly at the higher ion energies.

The effect of the mass of the substrate was examined, in order to attempt to resolve the difference between the findings of Winters and Webb and Meyerhoff. The technique used by Meyerhoff was again used in this study, except that the sputtering cross section of nitrogen was evaluated at three adatom placements as opposed to one, and the hit, no-hit cases were examined separately.

B. MOLYBDENUM RESULTS

1. Nitrogen Sputtering Cross Sections and Adatom Placement.

a. 500 eV Ion Bombardment

The sputtering of nitrogen as a function of adatom placement was examined at two energy levels, 500 eV and 2 keV. In addition, the "hit" and "no-hit" cases were examined separately. Table 10 lists the nitrogen sputter yield, and cross section as a function of adatom placement for the 500 eV bombardment. The results are plotted in Figure 11 for the hit, no-hit and total cross sections. The plot of cross section vs atom placement results in an apparent "well" corresponding to an adatom placement at 0.245 A above the (100) surface. This was true for both the hit and total cross section cases. The sputtering yield then increased as a function of adatom distance from the surface. The simulation cross section at this point is 5.63×10^{-16} cm^2, corresponding to the experimental value obtained by Winters of 5.6×10^{-16} cm^2.

The effect of the ion hitting the nitrogen is quite apparent. The sputtering cross section of the hit case increased by a factor of from 2 to 4 above the non-hit case, and by a factor of about 1.5 for the total cross section. This indicates that the primary mechanism for the sputtering of the nitrogen is when the incident ion hits the adatom, and it in turn is reflected from the substrate, as illustrated earlier in Figure 2(a). This seems to be more pronounced as the adatom is placed further above the "well" at .245 A. The agreement between the experimental and simulation results for this point indicates that the nitrogen may be located at approximately that height above the (001) surface. The nitrogen yields and cross sections are listed below

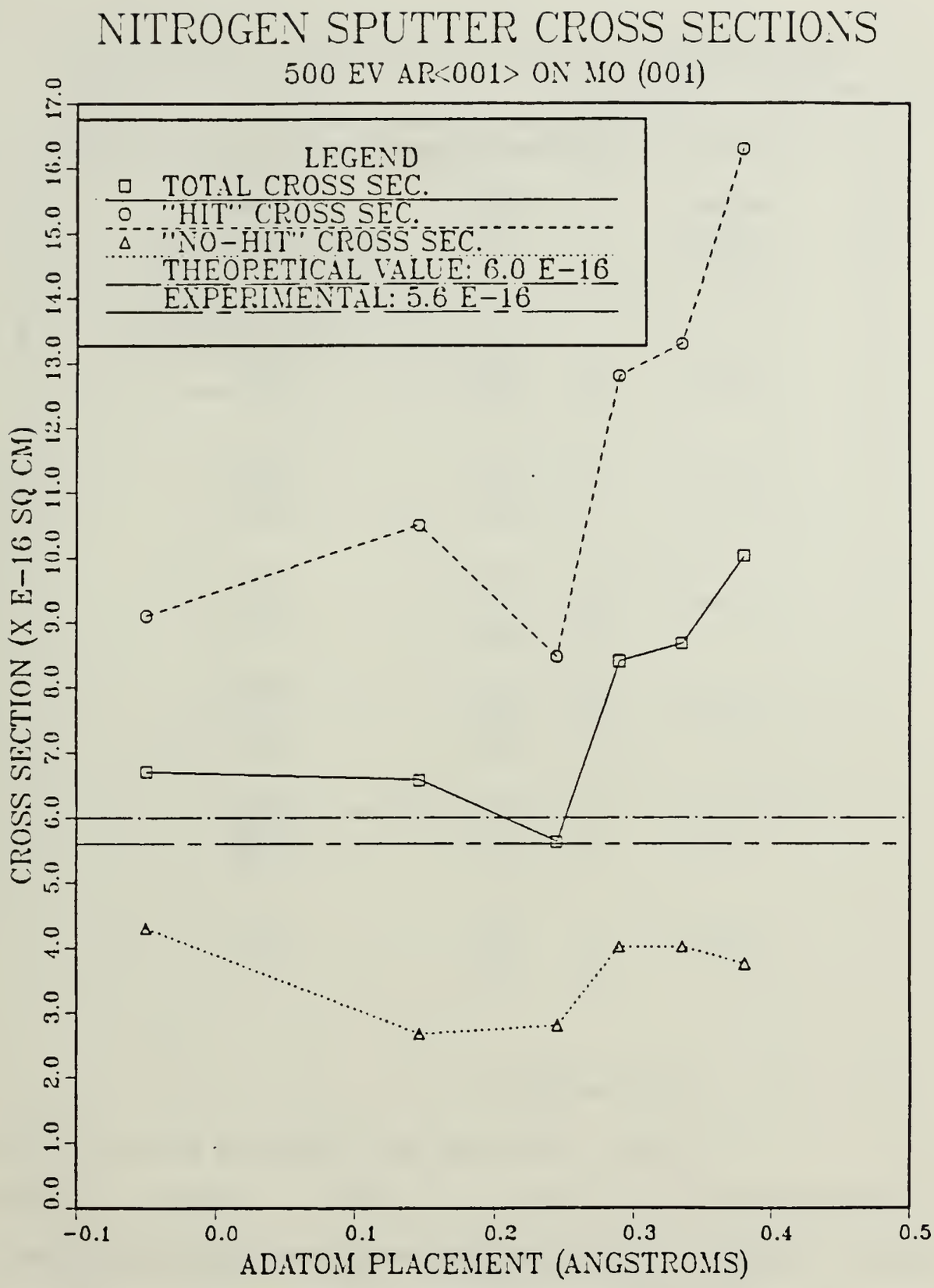

Figure 11. Comparison of "Hit", "No-hit" and Total Cross Sections With Theory and Experimental Values for 500 eV Ar on Molybdenum.

with H corresponding to the "hit" case, N for the "no-hit" case, and T for the total values.

TABLE 10. NITROGEN SPUTTERING DATA, Mo(001), 500 eV

Adatom Placement (A)		Sputter Yield	Cross Section ($\times 10^{-16}$ cm^2)
	H	0.41	9.1
-0.05	N	0.15	4.3
	T	0.28	6.7
	H	0.52	10.5
0.146	N	0.13	2.68
	T	0.33	6.57
	H	0.42	8.47
0.245	N	0.14	2.81
	T	0.28	5.63
	H	0.63	12.8
0.290	N	0.20	4.02
	T	0.42	8.4
	H	0.66	13.3
0.335	N	0.20	4.02
	T		8.67
	H	0.81	16.3
0.380	N	0.19	3.75
	T	0.50	10.02

b. 2 keV Bombardment

Nitrogen sputtering when bombarded at 2 keV was examined at the same adatom locations, and the data is tabulated in Table 11. Figure 12 shows the nitrogen sputtering cross sections as a function of adatom location, with the hit and no-hit case considered at four locations. The curves follow the same general trends as Figure 11, with some exceptions. The same "well" is observed, but in this case, the total

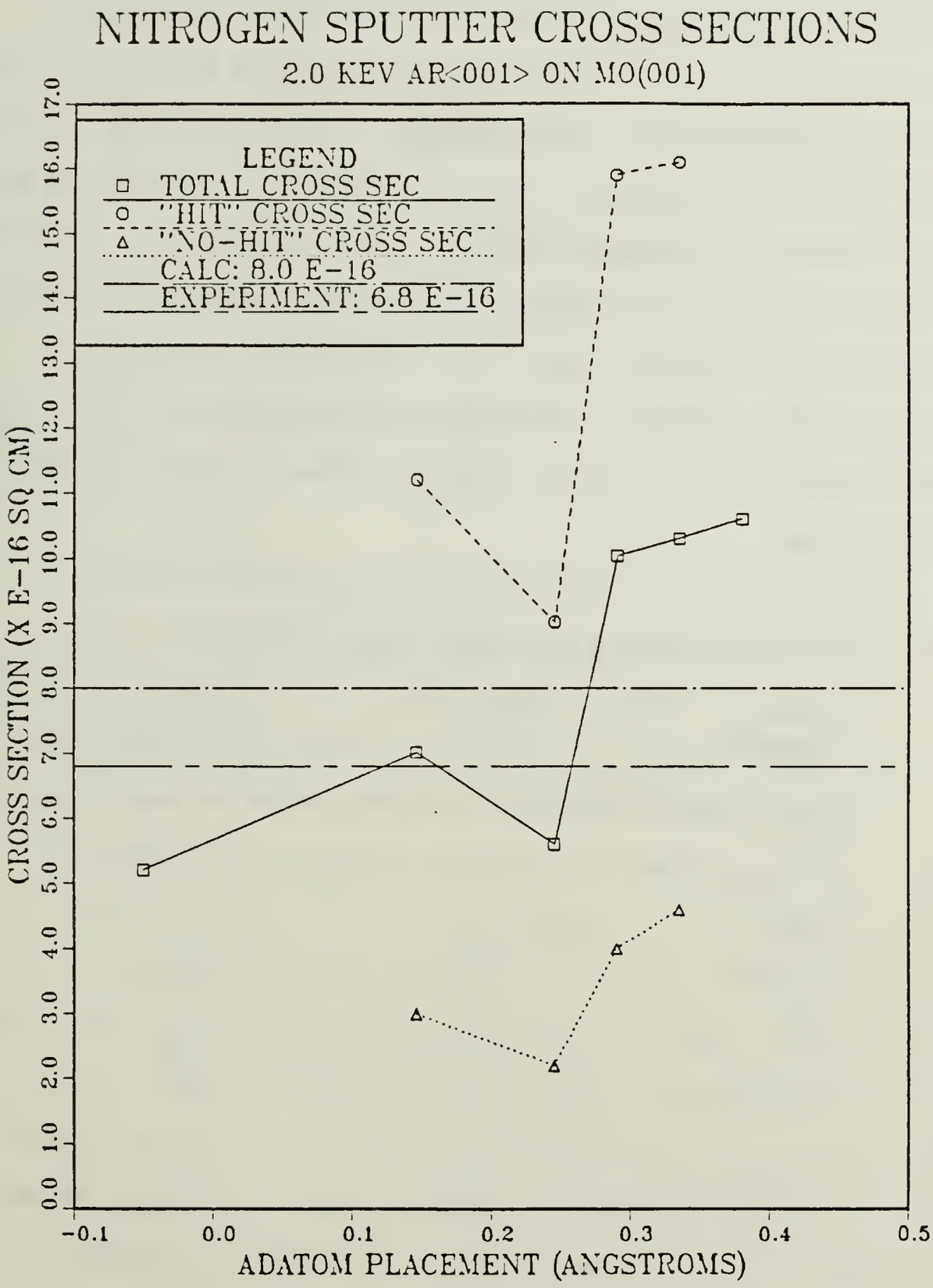

Figure 12. Comparison of "Hit", "No-hit" and Total Cross Sections With Theory and Experimental Values for 2 keV Ar on Molybdenum.

cross section of 5.6×10^{-16} cm^2 is below the experimental and theoretical values of 6.8×10^{-16} cm^2 and 8.0×10^{-16} cm^2 respectively. The slope of the sputtering cross section curve seems to level out at adatom placements above 0.29 A. The cross section for the -0.05 placement is below the "well" at 0.245 A. The -0.05 point was plotted using Webb's data. Both he and Meyerhoff used ^{14}N in their computations, where ^{15}N was used in this study, and in the experiments by Winters. The 7% mass difference may account for part of the difference in the result. The effect of the hit case is again quite apparent, with significantly higher sputter cross sections resulting from the ion striking the nitrogen atom.

TABLE 11. Mo-N SPUTTERING CROSS SECTIONS, 2.0 keV

Adatom Placement (A)		Sputter Yield	Sputter Cross Section (X 10^{-16} cm^2)
-0.05	T	0.26	5.2
	H	0.56	11.2
0.146	N	0.15	3.0
	T	0.35	7.01
	H	0.45	9.02
0.245	N	0.11	2.2
	T	0.28	5.6
	H	0.79	15.9
0.290	N	0.20	4.0
	T	0.50	10.03
	H	0.80	16.1
0.335	N	0.23	4.60
	T	0.51	10.3
0.380	T	0.53	10.6

c. Comparison of the Sputtering Cross Sections

The total sputtering cross sections for 500 eV and 2 keV are plotted on the same graph in Figure 13. The general trends are apparent. Both curves exhibit the same "well" corresponding to an adatom placement of 0.245 A. The sputtering cross sections then increase as a function of increasing height of adatom placement. There seems to be something special about the 0.245 A placement. Since the simulation cross section agreed so closely with the experiment, it is a good indication that this might be close to the actual location of the atom. The fact that the 2 keV curve so closely matches the 500 eV curve gives further credence to this assumption.

2. Nitrogen Sputtering Cross Sections as a Function of Energy

The sputtering of nitrogen as a function of energy was examined. The purpose of this analysis was to compare the results of the simulation to the data presented by Winters as listed in Table 9. Points were obtained at four energy levels, 500 eV and 1.0, 2.0, and 3.0 keV. The analysis was conducted for adatom placement at 0.245 A. This point was chosen, since it so closely matched the experimental cross section as mentioned above. The results are shown in Figure 14, with the corresponding experimental and theoretical values from Winters' paper. The values at 500 eV and 3.0 keV are within the bounds of the experimental and theoretical values, but the points at 1 keV and 2 keV are beyond the limits. The variation of the simulation results from those of Winters is a measure of the uncertainty of the simulation model. However, the general trend of the simulation cross sections do correlate with Winters' results.

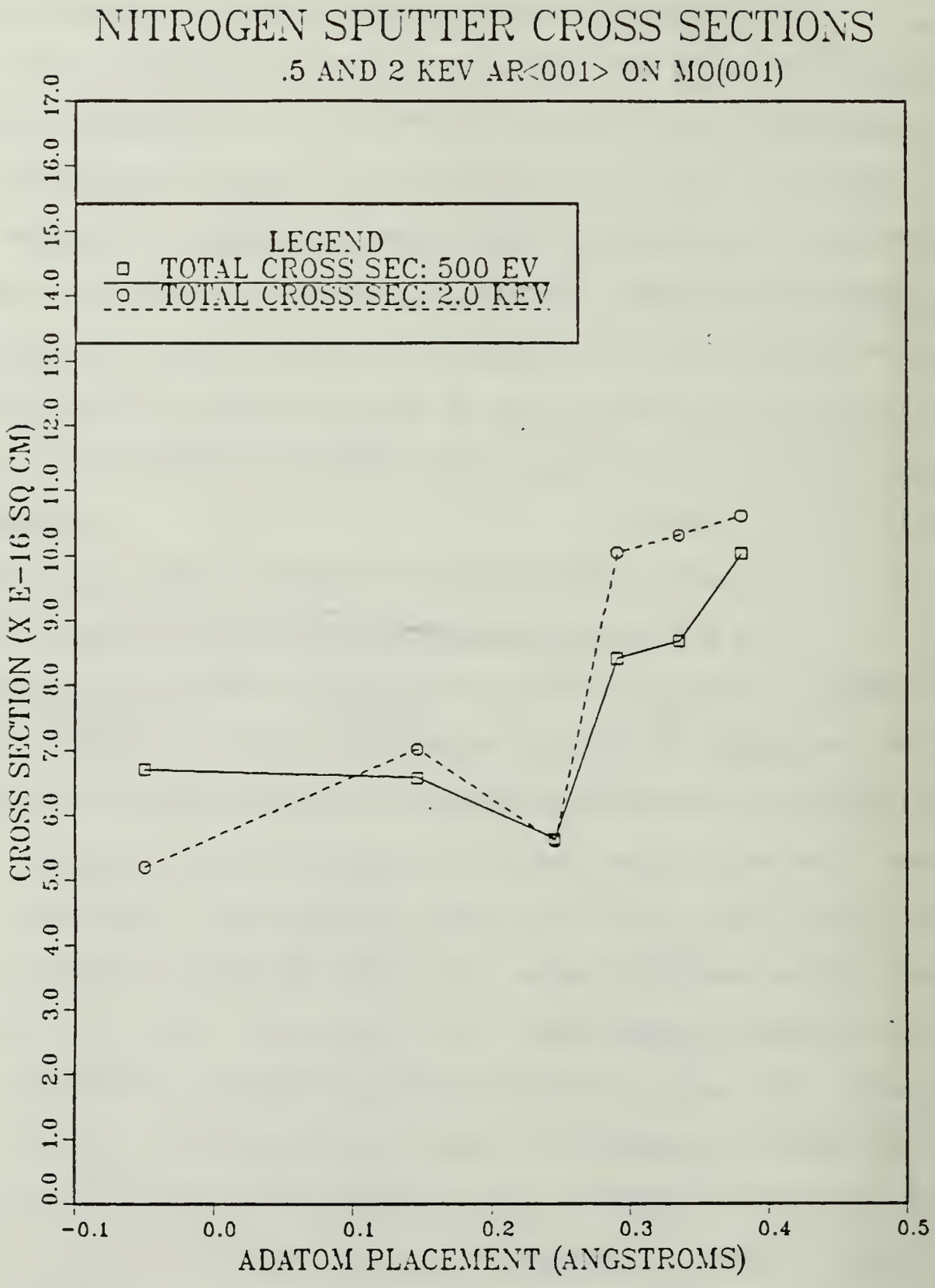

Figure 13. Comparison of Total Cross Sections for 500 eV and 2 keV Ar on Molybdenum.

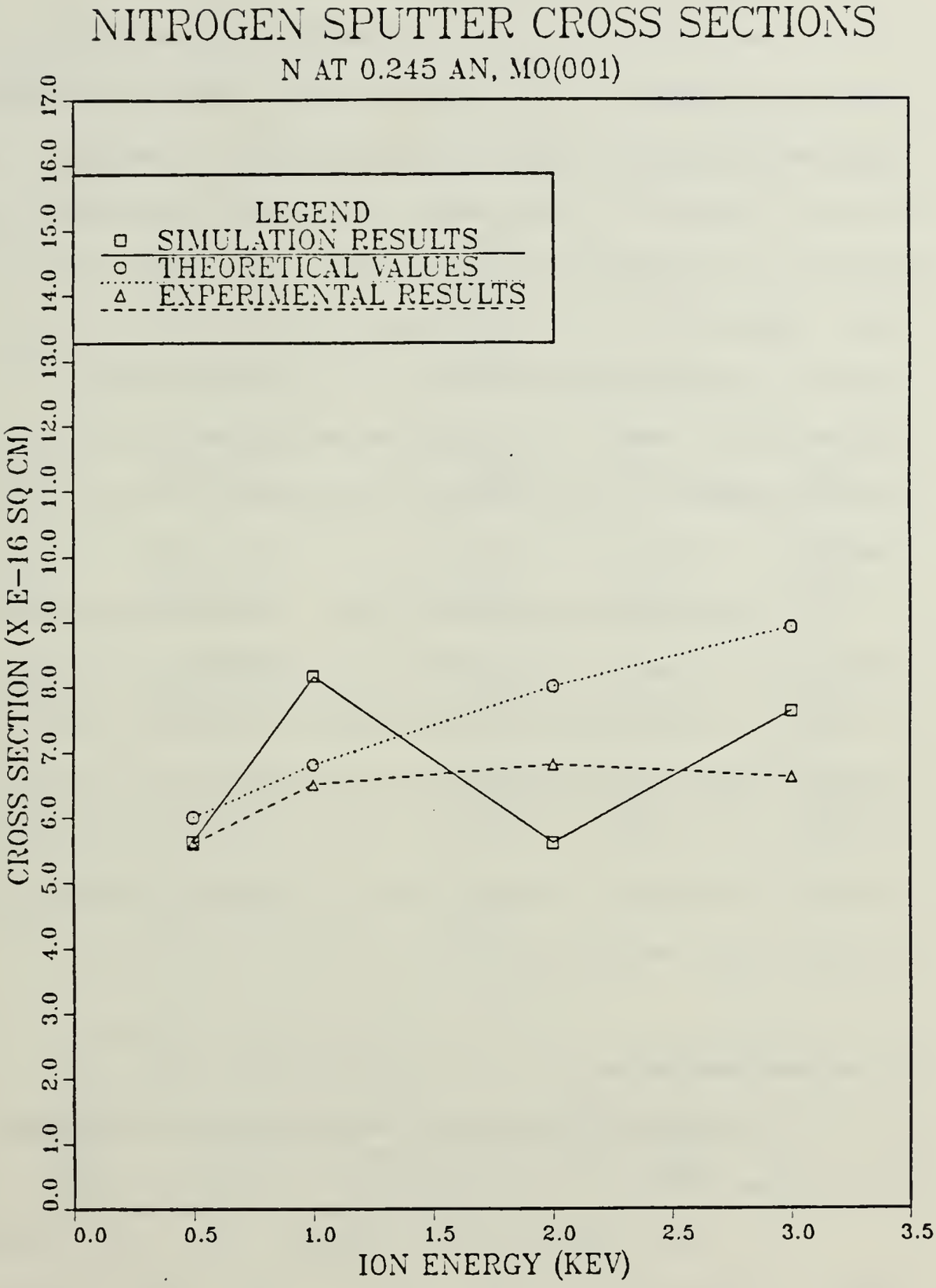

Figure 14. Nitrogen Sputtering Cross Section as a Function of Energy for Adatoms Placed at 0.245 A on Mo(100).

3. Sputtering of the Substrate

The ratio of the reacted substrate yield to the bare substrate yield was examined at 500 ev and 2 keV. The hit, no-hit and total yields were considered. The results are listed in Table 12, and are plotted in Figure 15. In all cases, for all adatom placements examined, the yield of the reacted surface was lower than that of the bare surface. Additionally, the substrate yields of the hit case were lower than for the total and non-hit case. This indicates that the nitrogen adatoms absorb some of the energy of the incident particle, and therefore less momentum is available to initiate the collision cascade in the substrate.

The case was the same at 2 keV. The sputtering yields of the substrate were lower in each case when the adatom was initially struck by the ion. The incident ion at 2 kev still failed to have sufficient energy to impart enough momentum to the adatom for it to act as a second projectile and thereby enhance the sputter yield of the substrate. The yields of the substrate and the ratios with the bare substrate for 2 keV are also listed in Table 12.

C. TUNGSTEN RESULTS

1. Nitrogen Sputtering Cross Sections and Adatom Placement

a. 500 eV Ion Bombardment

The sputtering of nitrogen from (001) tungsten was examined at 500 eV and 2 keV. The hit and no-hit scenarios were examined as with molybdenum. The results are listed in Table 13, and

TABLE 12. SPUTTER YIELD OF SUBSTRATE, Mo(100)

Adatom Placement (A)		500 eV Yield	500 eV Y_N/Y_B	2 keV Yield	2 keV Y_N/Y_B	
Bare	H	3.16	NA			
	N	3.41	NA			
	T	3.28	NA	3.02	NA	
-.05	H	1.99	0.630			
	N	2.29	0.671			
	T	2.14	0.652	2.29	0.76	
0.146	H	1.81	0.573	2.01	0.67	
	N	2.37	0.695	3.07	1.02	*
	T	2.09	0.637	2.54	0.84	
0.245	H	1.91	0.604	1.85	0.61	
	N	2.45	0.718	2.66	0.88	
	T	2.17	0.661	2.25	0.74	
0.290	H	2.03	0.642	2.28	0.75	
	N	2.51	0.736	3.15	1.04	*
	T	2.27	0.692	2.72	0.90	
0.335	H	2.08	0.658	2.09	0.69	
	N	2.60	0.762	3.17	1.05	*
	T	2.34	0.713	2.63	0.87	
0.380	H	2.03	0.642			
	N	2.59	0.760			
	T	2.31	0.704	2.25	0.74	

** It should be noted that the results for the bare substrate were taken from reference 50. The 2 keV Mo-bare case was not re-run. This could be part of the reason for the ratio of sputter yields for the new potential functions to be greater than 1. It does not seem reasonable that the yield of the reacted substrate should be greater than the bare substrate when the adatom is not struck.

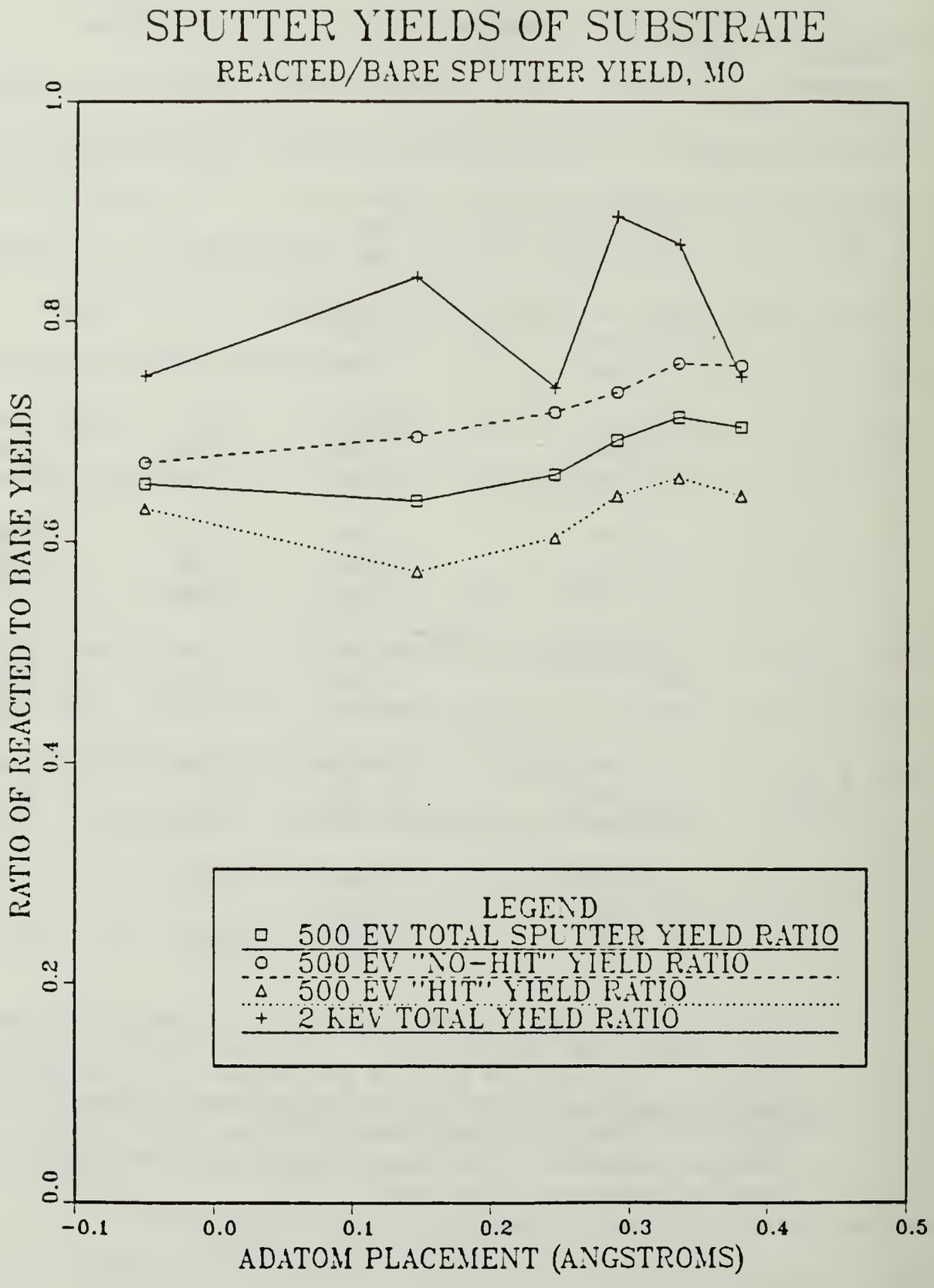

Figure 15. Ratio of the Sputter Yield of the Reacted Substrate to the Yield of the Bare Substrate.

are plotted in Figure 16. The same general pattern was found as for molybdenum. The sputtering cross section for the hit scenario is again significantly greater than for the no-hit case, for all adatom placements. Therefore, as with molybdenum, the majority of the nitrogen is sputtered as a result of a direct collision by the incident ion. The total sputtering cross sections generally follow the experimental values until the point corresponding to the 0.2464 A adatom location, where the slope of the cross section plot rapidly increases.

b. 2 keV Ion Bombardment

The sputtering cross section and yield data for the 2 keV bombardment is summarized in Table 14 and plotted in Figure 17. There is no "well" as was observed for the molybdenum case, however there is a break in the slope of the curve at the point corresponding to adatom placement at 0.2464 A. While not plotted, the sputtering cross sections for the hit case were again significantly greater in all instances than for the non-hit case.

c. Comparison of Sputtering Cross Sections

The total nitrogen sputtering cross sections for the 500 eV and 2 keV bombardments are plotted in Figure 18. The two curves follow the same general trends. A "well" is not observed, but there is an inflection point in the curves at a point corresponding to an adatom placement of 0.2464 A. One special note, the sputtering cross section

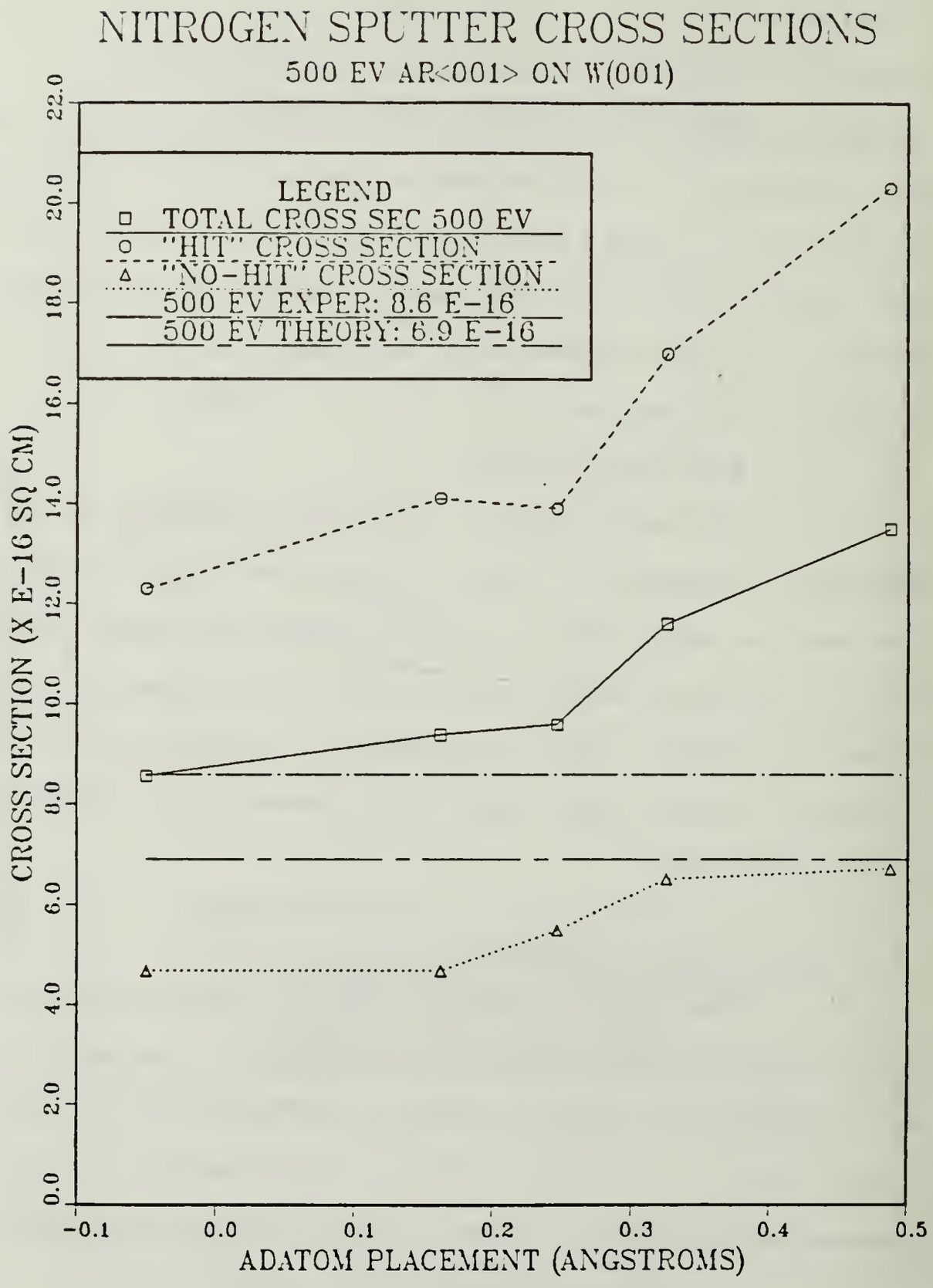

Figure 16. Comparison of Hit, No-hit and Total Nitrogen Sputtering Cross Section with Experiment and Theory for 500 eV Argon on W(100)

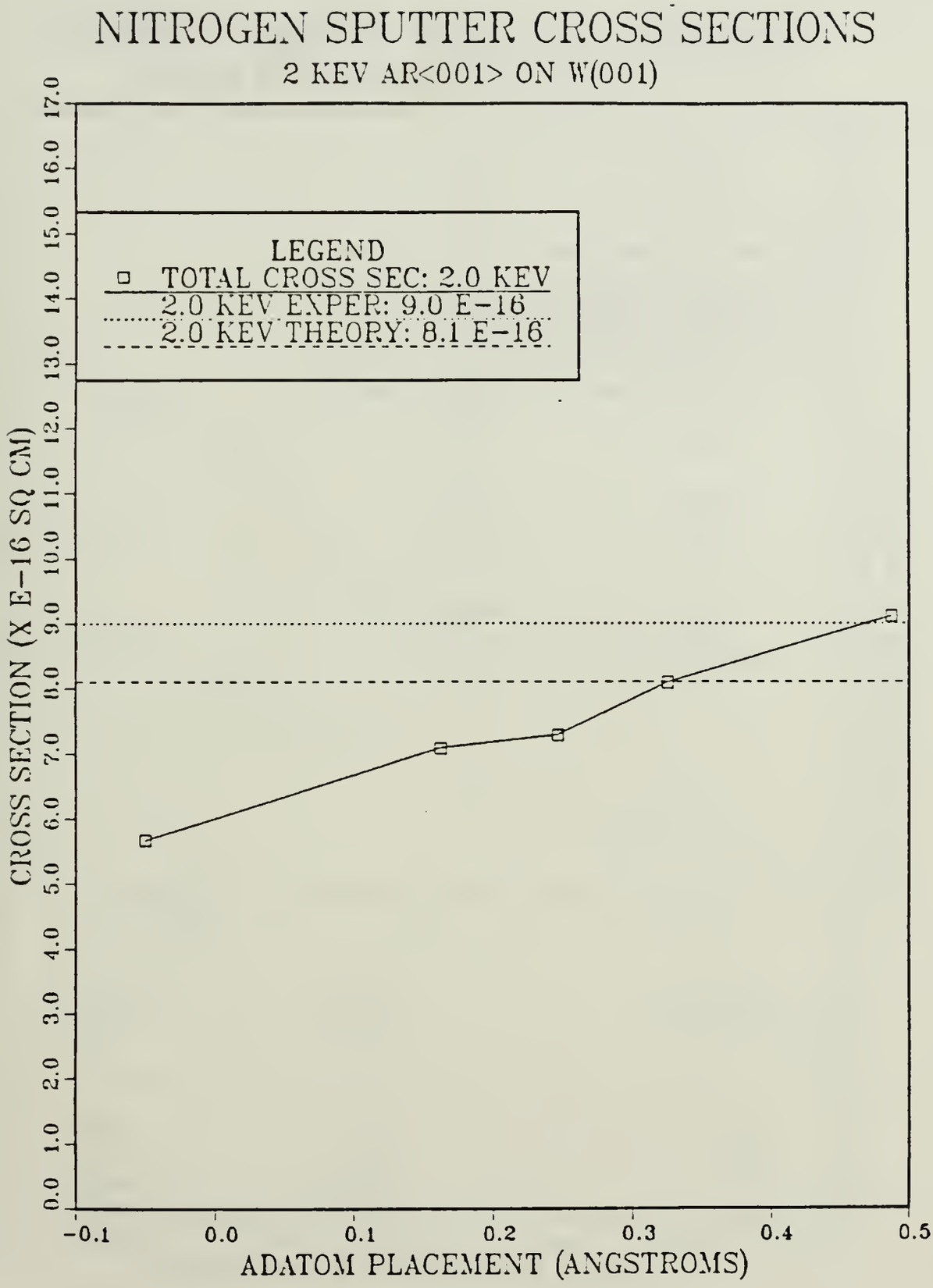

Figure 17. Nitrogen Sputtering Cross Section as a Function of Adatom Placement for 2 keV Argon on W(100).

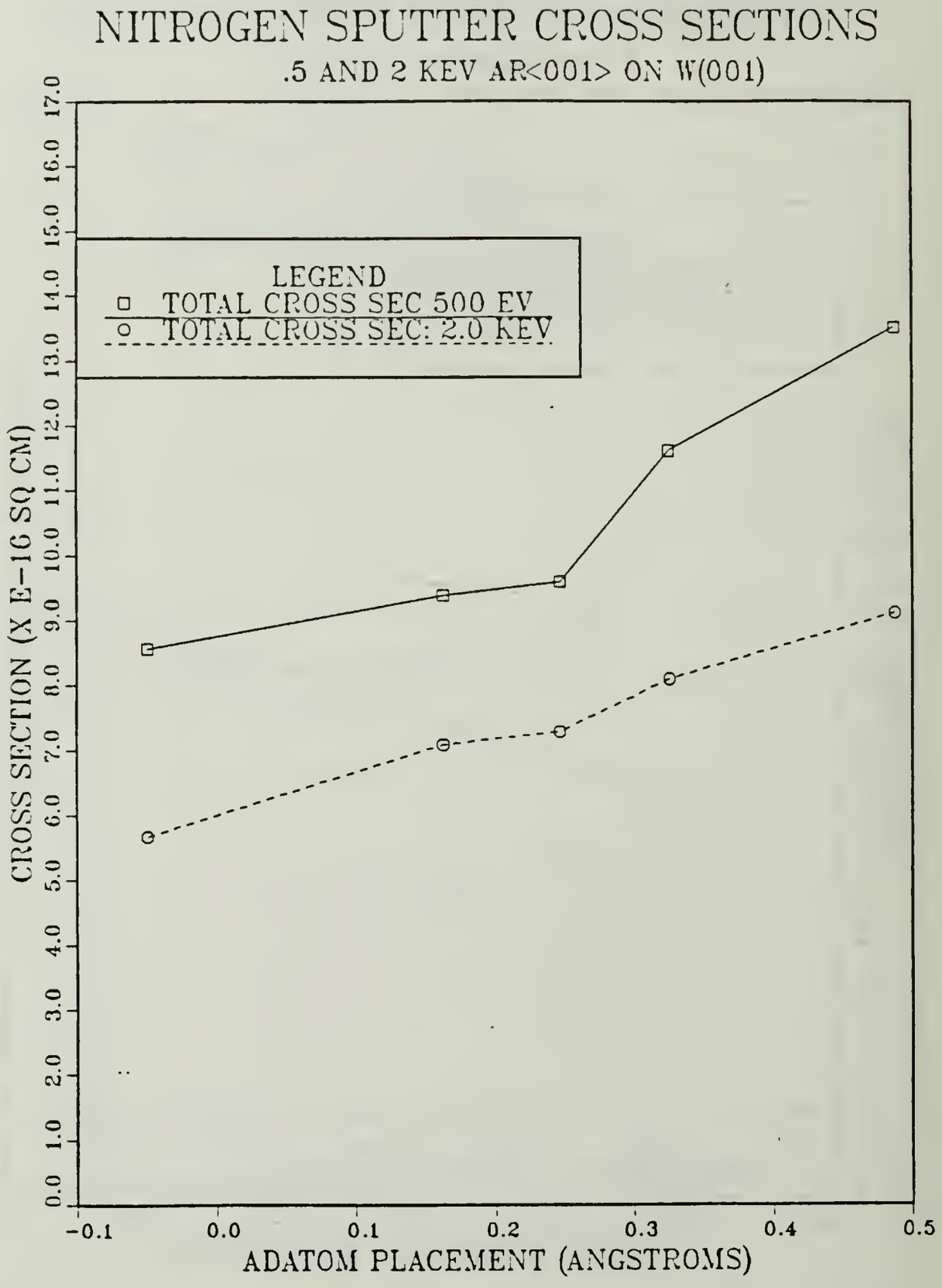

Figure 18. Comparison of Total Nitrogen Sputtering Cross Sections for 500 eV and 2 keV Argon on W(100).

TABLE 13. W(100) NITROGEN SPUTTERING RESULTS, 500 eV

Adatom Placement (A)		Sputter Yield	Sputter Cross Section ($\times 10^{-16}$ cm^2)
-.05	H	0.60	12.3
	N	0.23	4.68
	T	0.42	8.56
0.1623	H	0.69	14.1
	N	0.23	4.68
	T	0.46	9.38
0.2464	H	0.68	13.9
	N	0.27	5.49
	T	0.47	9.59
0.325	H	0.83	17.0
	N	0.32	6.51
	T	0.57	11.6
0.487	H	0.99	20.3
	N	0.33	6.72
	T	0.66	13.5

TABLE 14. NITROGEN YIELD AND SPUTTERING CROSS SECTIONS FROM TUNGSTEN 2.0 keV

Adatom Placement (A)	Total Sputter Yield	Sputter Cross Section ($\times 10^{-16}$ cm^2)
-.05	0.28	5.67
.1623	0.35	7.08
.2464	0.36	7.28
.325	0.40	8.09
.487	0.45	9.11

of nitrogen at 500 eV is significantly greater than at 2 keV for all adatom placements. This is similar to the findings in the two previous theses [Ref. 49, 50]. This conflicts with the experimental and theoretical values presented by Winters. This is an indication that the model used in the simulation is not correctly portraying the behavior of the nitrogen-tungsten system.

2. Nitrogen Sputtering as a Function of Energy

In an effort to find an adatom placement location that agreed with the experimental results, the total nitrogen sputtering cross section was plotted as a function of energy for all five adatom locations tested. The results are shown in Figure 19. In all cases, there was a strong negative slope, that did not correspond well with the slight positive slope of the experimental and theoretical values. Again this corresponds to Webb's and Meyerhoff's findings. This indicates that the potential function may not be reflecting the true behavior of the nitrogen on the tungsten.

3. Sputtering of the Substrate

The analysis of the ratio of the sputtering yield of the reacted substrate to the bare substrate was not conducted to the same detail as with molybdenum. The results for the cases examined are summarized below in Table 15. In all cases, with the exception of the hit case for placement below the surface at 500 eV, the yield of the reacted substrate was lower than that of the bare substrate. This was the case both at 500 eV and 2 keV. This indicates that for these two levels, the adatoms again reduce the energy of the ion such that less momentum is transferred to the substrate, and the yield of the substrate is lowered.

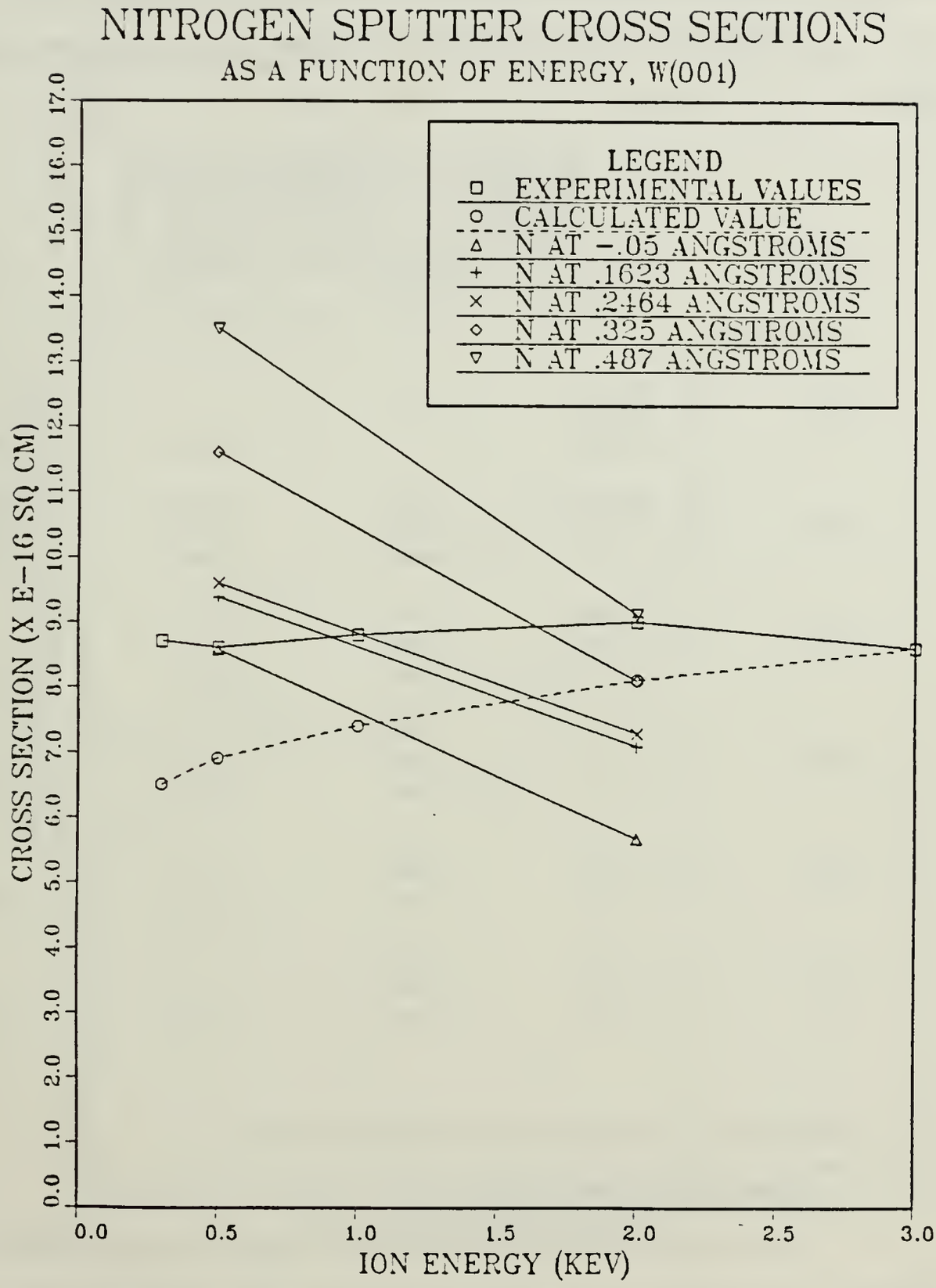

Figure 19. Comparison of Nitrogen Sputtering Cross sections as a Function of Energy and Adatom Location, W(100).

One interesting observation is that the yield of the substrate at 2 keV did increase, as expected, at the higher energy. This despite the fact that the simulation cross section of nitrogen sputtering was higher at 500 eV than at 2 keV.

TABLE 15. SPUTTER YIELD OF SUBSTRATE W(100)

Adatom Placement A		500 eV Yield	500 eV Y_N/Y_B	2 keV Yield	2 keV Y_N/Y_B
Bare	H	2.67			
	N	3.28	NA		
	T	2.98		2.63	NA
-0.05	H	1.79	0.67	2.16	0.82
	N	1.75	0.53	1.57	0.60
	T	1.77	0.59	1.87	0.71
0.1623	H	1.83	0.68		
	N	1.88	0.57		
	T	1.85	0.62	2.06	0.78
0.2464	H	1.77	0.67		
	N	1.9	0.57		
	T	1.84	0.62	2.35	0.89
0.325	H	1.76	0.66		
	N	2.05	0.63		
	T	1.90	0.64	2.50	0.95
0.487	H	1.73	0.65		
	N	2.23	0.68		
	T	1.98	0.66	1.96	0.74

D. COMPARISON OF MOLYBDENUM AND TUNGSTEN RESULTS

1. Comparison of Cross Sections

The sputtering cross sections of nitrogen from molybdenum and tungsten are plotted in Figure 20, with the adatom placement normalized to lattice units. The molybdenum curves exhibit the "well" at 0.156 LU,

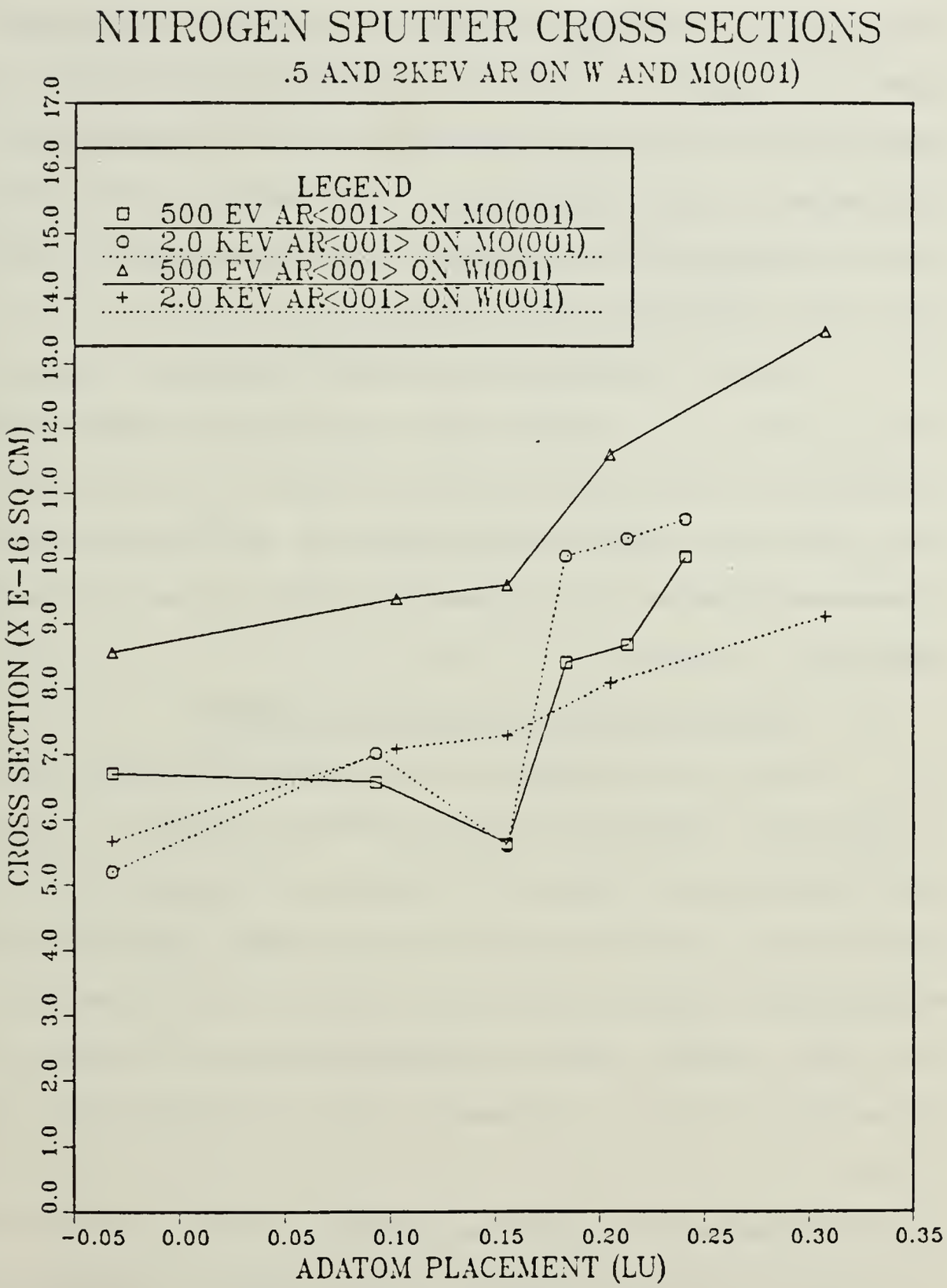

Figure 20. Comparison of Nitrogen Sputtering Cross Sections for Mo(100) and W(100) at 500 eV and 2 keV, Adatom Placement Normalized to Lattice Units.

but the tungsten curves show a definite "break" in slope at the same relative point. This point corresponds to 0.245 A for molybdenum, and 0.2464 A for tungsten. The potential function for the 0.2464 LU placement was derived so that the behavior at the point corresponding to the molybdenum well could be examined. Again the major difference between the two substrates is the fact that the sputtering cross section at 500 eV is higher than at 2 keV for tungsten.

The hit and no-hit analysis was conducted for tungsten also, and the same general trend was noted. Significantly higher sputtering cross sections were noted for the hit scenario. This was true at all energy levels and adatom placements examined. This indicates that the primary mechanism for the sputtering of nitrogen is due to direct collision by the incident ion.

2. Comparison of Substrate Sputtering Yields

The ratios of the sputtering yields of the reacted substrates to the bare substrates at 500 eV and 2 keV bombardments indicate that the nitrogen does not enhance the sputtering of the substrate. This is observed even at the relatively high energy level of 2 keV. Both molybdenum and tungsten exhibited this behavior. The incident ion, even at 2 keV failed to transfer enough momentum to the nitrogen for it to act as a second projectile to enhance the sputtering of the substrate.

E. DETERMINATION OF POSSIBLE MASS EFFECTS

One of the major conclusions in Winters' earlier works was the fact that the sputtering cross section seemed to be greater for the substrate with the higher mass [Ref. 48, 55]. Meyerhoff and Webb examined this

aspect, and concluded that adatom placement had a greater effect. The mass effect was examined in this thesis by selecting three adatom locations in the vicinity of the "well" at 0.245 A, for the Mo(100) surface, and replacing the mass of the molybdenum with the tungsten mass, leaving all other aspects of the potential functions the same. The results are plotted in Figure 21, for the hit, no-hit and total cross section cases. In all cases, the sputtering cross sections were higher for the higher mass. This indicates that the mass of the substrate does have an effect on the sputtering cross section of the nitrogen.

Figure 22 shows the total nitrogen sputtering cross sections for 500 eV Mo(100), Mo*(100) (the high-mass molybdenum), and W(100). The graph is normalized for adatom placements at approximately corresponding locations. The trend for higher sputter cross sections for the higher mass is obvious. The heavy Mo* has higher nitrogen sputtering cross sections than the true molybdenum, and the tungsten has the highest cross sections of the three. Through the use of the computer simulation, the mass effects have been able to be truly isolated, more so than is possible in a physical system. This is one valuable aspect of simulations.

One possible reason for the higher sputtering cross section for the heavier substrate is that the greater mass of the substrate provides a better "springboard" for the nitrogen atoms. When the nitrogen atoms are knocked from their positions by the incident ions, they relatively light nitrogen atoms will rebound with more initial momentum conserved from the heavier tungsten atoms than from the lighter molybdenum atoms.

This model for the increase in sputtering yield with higher substrate mass follows if the primary mechanism for the sputtering of the

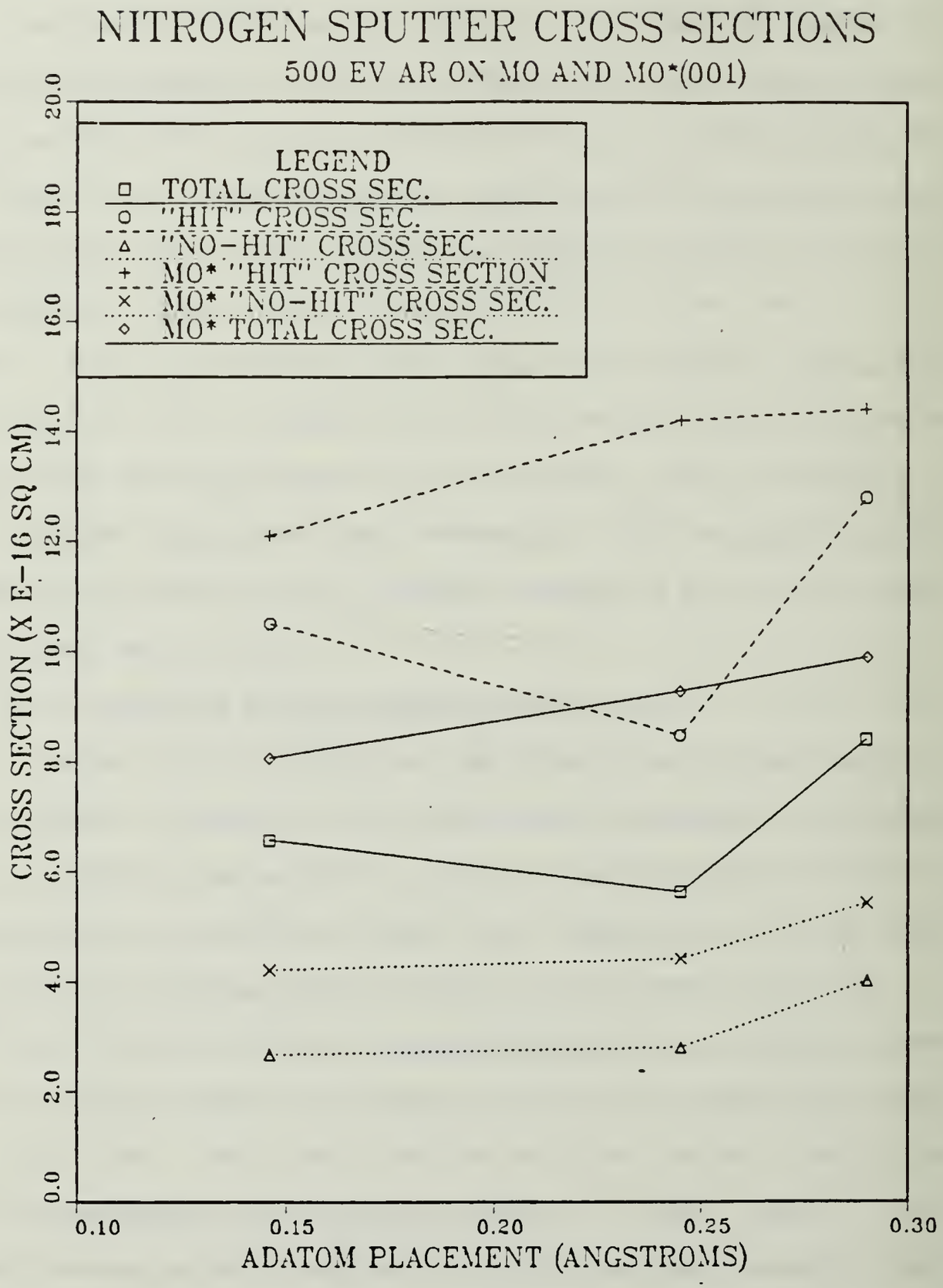

Figure 21. Comparison of Nitrogen Sputtering Yields for Mo(100) and Mo*(100), 500 eV Argon.

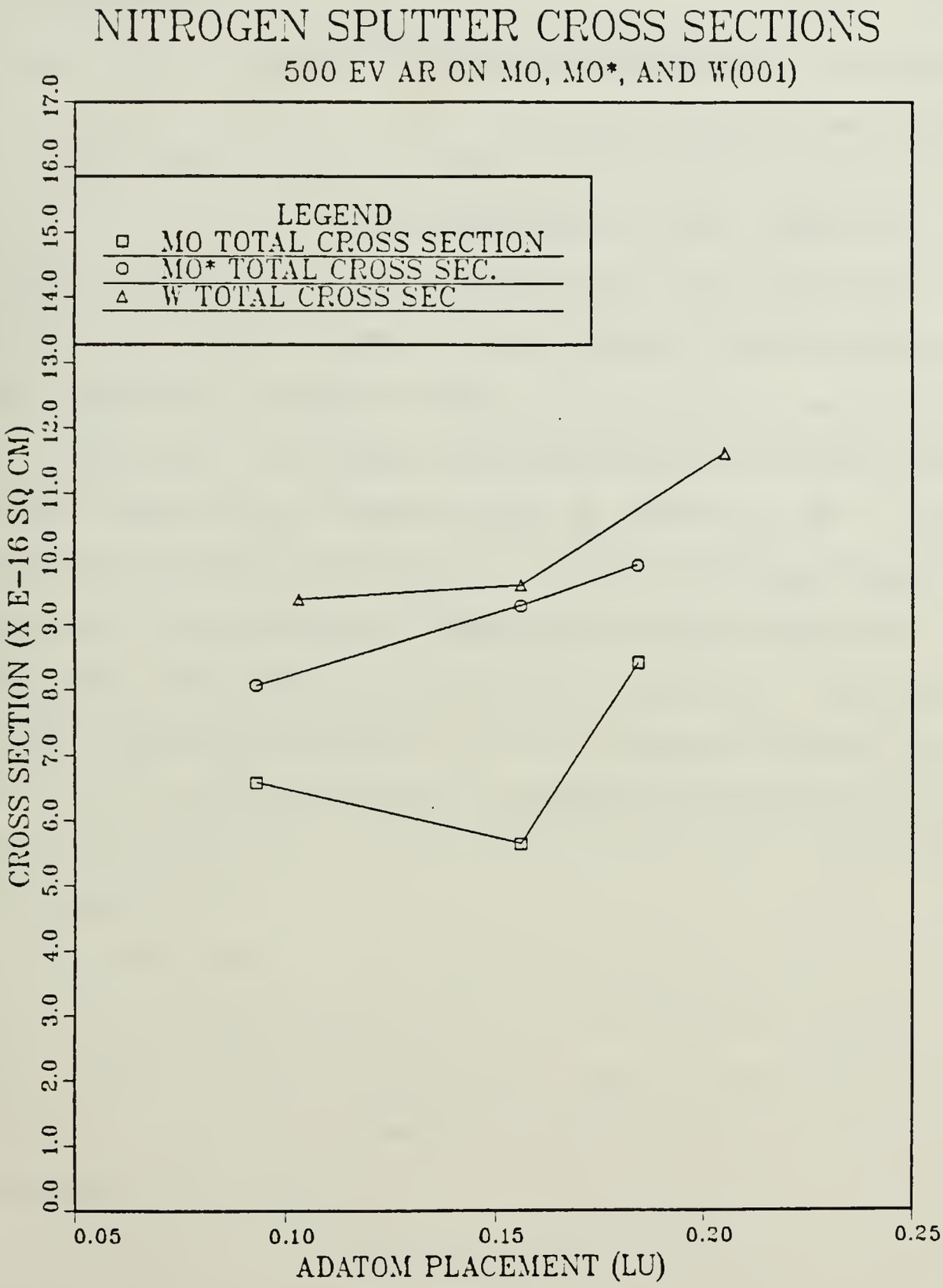

Figure 22. Comparison of Total Nitrogen Sputtering Cross Sections for Mo(100), Mo*(100), and W(100), 500 eV Argon.

nitrogen is direct collision by the incident ion. If the nitrogen atoms were knocked off by reflected argon ions, or by sputtering substrate materials to a high degree, the effect of the mass of the substrate would seem to be less important.

F. COMPARISON WITH PREVIOUS SIMULATIONS

The results of this study indicates that there is a significant mass effect, this is contrary to the findings of Webb and Meyerhoff. The earlier studies did not isolate the effects of the direct interaction of the ion with the adatom to the degree that it was done in this study. The trend for the higher nitrogen sputtering cross section at the lower energy for tungsten is consistent through the three studies.

The other aspects of the computer simulation, such as the angular and energy distribution plots remained consistent with earlier works. For a more detailed analysis of the "traditional" sputtering simulation analysis, the reader is referred to References 49 and 50.

V. CONCLUSIONS AND RECOMMENDATIONS

The results of this simulation confirm the findings of Webb and Meyerhoff that the placement of the adatoms is most likely above the crystal surface. A location of approximately 0.245 A for the molybdenum surface results in a nitrogen sputtering cross section that agrees with the experimental results of Winters.

Comparison of the "hit" and "no-hit" scenarios indicates that the primary mechanism for the sputtering of the adatom is due to direct collisions with the incident ion. In all cases examined, the sputtering cross sections derived when the adatom was struck by the incident ion were larger than in the cases when they were not struck. This was found at both energy levels examined, 500 eV and 2 keV; and for both Mo(100) and W(100). This agrees partially with Winter's conclusions, but does not show a significant increase in non-hit sputtering at higher energies he proposed.

The mass effect of the substrate was examined, and it was determined that the sputtering cross section of the adatom was enhanced with the increase of mass of the substrate, when all other factors are held constant. This contradicts Meyerhoff's findings, but only one point was considered in his analysis.

The ratio of the sputtering yield of the bare substrate to the reacted substrate was evaluated for both systems. The analyses indicated that the adatoms decrease the amount of energy imparted to the

substrate, and reduces the sputter yield for the "hit" case. This momentum loss was observed at 500 eV and 2 keV. This process could change at higher energy levels (greater than 2 keV) of the incident particles.

A significant difference was found for tungsten between the simulation and experimental and theoretical sputtering cross sections. The nitrogen sputtering cross section for the 500 eV bombarding energy was higher than for the 2 kev energy, which was in contradiction to Winter's results. A similar finding was made by Webb. This indicates that perhaps the pair potentials used to model the nitrogen on tungsten are not correct. It has been determined that the oxygen-tungsten system behaves quite differently than the oxygen-molybdenum system, so perhaps this trend continues for the Mo-N and W-N systems [Ref. 67].

Further simulation studies should be made to complete the comparison with Winters' study. Studies should be made using helium and xenon ions in order to investigate the effect of the mass of the incident ion. Additional studies should be conducted on tungsten to determine if the lower sputtering cross section at 2 keV was due to nitrogen atoms being captured as interstitials in the tungsten lattice, or if there is a defect in the potential functions. Higher energy studies should be conducted to identify the point at which the sputtering yield of the substrate will be enhanced by the adatoms.

APPENDIX

DERIVATION OF SPUTTERING CROSS SECTIONS

The methodology used for the derivation of the sputtering cross section in this thesis is based on the technique used by Winters in reference 55. The notation used in this appendix closely parallels that of Winters.

The rate that nitrogen is sputtered from the surface of the target is given by the relation:

$$-R_N = \frac{d\Theta_N}{dt} = -\sigma \Theta_N \nu^+ t \quad , \qquad (7)$$

where the following are defined:

$R_N \equiv$ the nitrogen sputtering rate, {atoms / cm^2 - sec};
$\Theta_N \equiv$ the nitrogen atom concentration at time = t, {atoms / cm^2};
$\sigma \equiv$ the sputtering cross section, {cm^2};
$\nu^+ \equiv$ the incident ion flux, {ion / cm^2 - sec};
$t \equiv$ the time in seconds, {sec}; and
$\nu^+ t \equiv$ the ion dose, (fluence), {ion / cm^2}.

Solving equation 7 yields,

$$\ln (\Theta_N / \Theta_{No}) = -\sigma \nu^+ t, \qquad (8)$$

where $\Theta_{No} \equiv$ the initial nitrogen concentration at t = 0. Rearranging equation 8, and solving for σ results in the following relation for the cross section;

$$\sigma = -\ln (\Theta_N/\Theta_{No}) / \nu^+ t \ . \qquad (9)$$

The Θ_N/Θ_{NO} term is next examined. The following relations are defined,

No ≡ the number of nitrogen atoms on the surface at t = 0,
NTRAJ ≡ the number of trajectories run, also
NTRAJ ≡ the number of incident ions on the target,
NSPUTT ≡ the number of nitrogen atoms sputtered from the surface,
A_O ≡ the area of the target $\{cm^2\}$.

Consequently, for each trajectory we have

$$\Theta_N = (N_O - NSPUTT) / A_O,$$

and $\Theta_{NO} = N_O/A_O$. Thus,

$$\frac{\Theta_N}{\Theta_{NO}} = \frac{(N_O - NSPUTT) / A_O}{N_O / A_O} = \frac{(N_O - NSPUTT)}{N_O}$$

Summing over all trajectories,

$$\frac{\Theta_N}{\Theta_{NO}} = \sum_{i=1}^{NTRAJ} \frac{(N_O - NSPUTT)_i}{N_O}$$

$$= 1 - \frac{\sum_{i=1}^{NTRAJ} NSPUTT_i}{(N_O)\ (NTRAJ)}$$

If we define $\sum_{i=1}^{NTRAJ} NSPUTT = TOTSPUT$, then

$$\frac{\Theta_N}{\Theta_{No}} = 1 - \frac{TOTSPUT}{(N_o)\ (NTRAJ)} \quad . \qquad (10)$$

Incorporating the relation for the beam fluence, from equation 9 yields the following relation for the cross section;

$$\sigma = -\left\{ \ln\left(1 - \frac{TOTSPUTT}{(N_o)\ (NTRAJ)}\right)\right\} A_o,$$

but $\frac{TOTSPUTT}{NTRAJ} \equiv$ YIELD, so as a result;

$$\sigma = -\left\{ \ln\left(1 - \frac{YIELD}{N_o}\right)\right\} A_o \ . \qquad (11)$$

Equation 11 is the relation used to calculate the sputtering cross section for the adsorbed nitrogen from the tungsten and molybdenum surfaces.

LIST OF REFERENCES

1. Grove, W.R., "On the Electro-Chemical Polarity of Gases," Trans. Royal Society of London, v. 142, pp. 87-102, 1852.

2. Plucker, J., "Fortgesetzte Beobachtungen Uber die Elekthische Endladung durch Gasverdunnte Raume," Annalen der Physik, v. 104, p. 113, 1858.

3. Plucker, J., " Ueber die Einwirkung des Magneten auf die Elektrischen Entlandungen in Verdunnten Gasen," Annalen der Physik, v. 103, p. 88, 1858.

4. Plucker, J., "Fortgestezte Beobachtungen Uber die Elektrische Entladung," Annalen der Physik, v. 105, p. 67, 1858.

5. Gassiot, J.P., "On the Stratifications and Dark Bands in Electrical Discharges as Observed in Torricellian Vacua," Trans. Royal Society of London, v. 148, pp. 1-16, 1858.

6. Goldstein, E., "The Canal-Ray Group," Verh. Dtsch. Phys. Ges., v. 4, pp. 228-237, 1902.

7. Stark, J., "Volatilisation by Atom Rays," Zeitschrift fur Elektrochem., v. 15, pp. 509-512, 1909.

8. Thompson, J.J., Rays of Positive Electricity and Their Applications to Chemical Analyses, Longmans, Green and Co., 1921.

9. Bush, V. and Smith, C.G., "Control of Gaseous Conduction," Trans. of Amer. Inst. of Electrical Engineers, v. 41 pp.402-411, 1922.

10. Kingdon, K.H. and Langmuir, I., "The Removal of Thorium from the Surface of a Thoriated Tungsten Filament by Positive Ion Bombardment," Physical Review, v. 22, pp. 148-160, 1923.

11. Kingdon, K. H. and Langmuir, I., "The Removal of Thorium from the Surface of a Thoriated Tungsten Filament by Bombardment with Positive Ions," Physical Review, v. 20, p. 108, 1922.

12 Blechschmidt, E., "Die Kathodenzerstaubung in Abhangigkeit von den Betriebsbedingungen," Annalen Der Physik, v. 81, pp. 999-1042, 1926.

13. Blechschmidt, E. and von Hipple, A., "Der Einfluss von Material und Zustand der Kathode auf den Zerstaubungsprozess," Annalen der Physik, v. 86, pp. 1006-1024, 1928.

14. Von Hipple, A., "Über die Natur und den Ladungszustand der bei Kathodenzerstaubung Emittierten Metallteilchen," Annalen Der Physik, v. 80, pp. 672-706, 1926.

15. Von Hipple, A., "Zur Theorie der Kathodenzerstaubung," Annalen Der Physik, v. 81, pp. 1043-1075, 1926.

16. Lamar, E.S. and Compton, K.T., "A Special Theory of Cathode Sputtering," Science, v. 80, p. 541, 1934.

17. Penning, F.M. and Moubis, J.H.A., "Cathode Sputtering in a Magnetic Field," Koninkl. Ned. Akad. Wehenschap. Proc., v. 43, pp. 41-56, 1940.

18. Kewell, F., "A Mechanism for Sputtering in the High Vacuum Based on the Theory of Neutron Cooling," Physical Review, v. 87, pp. 160-161, 1952.

19. Wehner, G.K., "Momentum Transfer in Sputtering by Ion Bombardment," Journal of Applied Physics, v. 25, pp. 270-271, 1954.

20. Wehner, G.K., "Sputtering of Metal Single Crystals by Ion Bombardment," Journal of Applied Physics, v. 26, pp. 1056-1057, 1955.

21. Wehner, G.K., "Controlled Sputtering of Metals by Low Energy Hg Ions," Physical Review, v. 102, pp. 690-704, 1956.

22. Harrison, D.E., Jr., "Theory of the Sputtering Process," Physical Review, v. 102, pp. 1473-1480, 1956.

23. Behrisch, R., "Introduction and Overview," Sputtering by Particle Bombardment I, R. Behrisch, ed., pp. 1-8, Springer, 1981.

24. Townsend, P.D., Kelly, J.C., and Hartley, N.E.W., Ion Implantation, Sputtering and Their Applications, Academic Press, 1976.

25. Robinson, M.T., "Theoretical Aspects of Monocrystal Sputtering," Sputtering by Particle Bombardment I, R. Behrisch, ed., Springer, 1981.

26. Garrison, B.J., Winograd, N., and Harrison, D.E., Jr., "Atomic and Molecular Ejection from Ion-Bombarded Reacted Single-Crystal Surfaces. Oxygen on Copper(100)," Physical Review B, v. 18, pp. 6000-6010, 1978.

27. Winters, H.F. and Sigmund, P., "Sputtering of Chemisorbed Gas (Nitrogen on Tungsten) by Low Energy Ions," Journal of Applied Physics, v. 45, pp. 4760-4766, 1974.

28. Wood, E.A., "Vocabulary of Surface Crystallography," Journal of Applied Physics, v. 35, pp. 1306-1312, 1964.

29. Carter, G. and Colligon, J.S., Ion Bombardment of Solids, American Elsevier Publishing Co., Inc., 1968.

30. Sigmund, P., "Sputtering by Particle Bombardment: Theoretical Concepts," Sputtering by Particle Bombardment I, R. Behrisch ed., Springer, pp. 9-71, 1981.

31. Wehner, G.K., "Sputtering Yield Data in the 100-600eV Energy Range," General Mills Report 2309, 1962.

32. Wehner, G.K., Anderson, G.S., and KenKnight, C.E., Litton Industries Report 3031, Litton Systems, Inc., 1966.

33. Silsbee, R.H., "Focusing in Collision Problems in Solids," Journal of Applied Physics, v. 28, pp. 1246-1250, 1957.

34. Sigmund, P., "Theory of Sputtering I. Sputtering Yield of Amorphous and Polycrystalline Targets," Physical Review, v. 184, pp. 383-415, 1969.

35. Thompson, M.W., "The Energy Spectrum of Ejected Atoms During High-Energy Sputtering of Gold," Philosophical Magazine, v. 18, pp. 377-414, 1968.

36. Harrison, D.E., Jr., "Sputtering Models - A Synoptic View," Radiation Effects, v. 70, pp. 1-64, 1983.

37. Kelly, R., "The Mechanisms of Sputtering. Part I. Prompt and Slow Collisional Sputtering," Radiation Effects, v. 80, pp. 273-317, 1984.

38. Gibson, J.B., and others, "Dynamics of Radiation Damage," Physical Review, v. 120, pp. 1229-1253, 1960.

39. Robinson, M.T. and Torrens, I.M., "Computer Simulation of Atomic-Displacement Cascades in Solids in the Binary Collision Approximation," Physical Review B, v. 9B, pp. 5008-5024, 1974.

40. Webb, R.P. and Harrison, D.E., Jr., "Near-Threshold Sputtering Mechanisms from a Computer Simulation of Argon-Bombarded Clean and Oxygen-Reacted Copper Single Crystals," Journal of Applied Physics, v. 53, pp. 5243-5249, 1982.

41. Thompson, J.J. and Thompson, G.P., Conduction of Electricity Through Gases, third edition, Cambridge, 1928.

42. Loeb, L.B., Fundamental Processes of Electrical Discharge in Gases, Wiley, 1939.

43. Taglauer, E., "Atomic Collision Processes During Plasma-Wall Interaction in Fusion Devices," Nuclear Instruments and Methods in Physics Research, v. B13, pp. 218-224, 1986.

44. Johnson, L.F., "Ion Beam Microstructure Fabrication in Optical, Magnetic and Surface Acoustical Technologies," Ion Bombardment Modification of Surfaces, O. Auciello and R. Kelly, eds., Elsivier, pp. 361-397, 1984.

45. Banks, B.A., "Ion Bombardment Modification of Surfaces in Biomedical Applications," Ion Bombardment Modification of Surfaces, O. Auciello and R. Kelly, eds. Elsivier, pp. 399-434, 1984.

46. NASA, Sputtering and Ion Plating, A Conference Held at Lewis Research Center, Mar 16, 1972, NASA, 1972.

47. Alnot, P. and King, D.A., "Trapping, Sticking, and Reactive Scattering in Chemisorption: Nitrogen Isotopes on W(100)," Surface Science, v. 126, pp. 359-367, 1983.

48. Winters, H.F., "Mass Effect in the Physical Sputtering of Multicomponent Materials," Journal of Vacuum Science and Technology, v. 20, pp. 493-497, 1982.

49. Meyerhoff, D., Computer Simulation Studies of Sputtering From Clean Tungsten and Nitrogen Reacted Tungsten and Molybdenum Surfaces, Masters Thesis, Naval Postgraduate School, Monterey, California, December 1983.

50. Webb, S.M., Study of Computer Simulation of Sputtering from Nitrogen Reacted Molybdenum and Tungsten Targets, Masters Thesis, Naval Postgraduate School, Monterey, California, June 1986.

51. Clavenna, L.R. and Schmidt, L.D., "Interaction of N-2 with (100) W," Surface Science, v. 22, pp. 365-391, 1970.

52. Adams, D.L. and Germer, L.H., "The Adsorption of Nitrogen on W(100)," Surface Science, v. 26, pp. 109-124, 1971.

53. Adams, D.L. and Germer, L.H., "Adsorption on Single Crystal Planes of Tungsten I. Nitrogen," Surface Science, v. 27, pp. 21-44, 1971.

54. Griffiths, K., and others, "Adsorbate-Induced Contracted Domain Structure: Nitrogen Chemisorbed on W {001}," Physical Review Letters, v. 46, pp. 1584-1587, 1981.

55. Winters, H.F. and Taglauer, E., "The Sputtering of Chemisorbed Nitrogen From Single Crystal Planes of Tungsten and Molybdenum," IBM Research Report, 1986.

56. Winters, H.F., Schlaegel, J., and Horne, D., "RF Induction Technique for Sample Heating in Surface Science Experiments," Journal of Vacuum Science and Technology, v. 15, pp. 1605-1608, 1978.

57. Jakas, Mario M. and Harrison, D.E., Jr., "A Comparison Between Multiple Interaction Computer Simulations and the Linear Theory of Sputtering," Nuclear Instruments and Methods in Physics Research, v. B14, pp. 535-541, 1986.

58. Webb, R.P., Harrison, D.E., Jr., and Jakas, M.M., "The Computer Simulation of Ion Induced Atomic Collision Cascades," Nuclear Instruments and Methods in Physics Research, v. B15, pp. 1-7, 1986.

59. Harrison, D.E., Jr. and Jakas, M.M., "Simulation of the Atomic Collision Cascade," Radiation Effects, v. 99, pp. 153-169, 1986.

60. Chemical Rubber Company, Handbook of Chemistry and Physics, 54th ed, CRC Press, 1973.

61. Askland, D.R., The Science and Engineering of Materials, PWS Engineering, 1984.

62. Simons, Eric N., Guide to the Uncommon Metals, Hart, 1967.

63. General Electric, Chart of the Nuclides, 1975.

64. Harrison, D.E., Jr. and Webb, R.P., "A Molecular Dynamics Simulation Study of the Influence of the Lattice Atom Potential Function upon Atom Ejection Processes," Journal of Applied Physics, v. 53, pp. 4193-4201, 1982.

65. Huber, K.P. and Herzberg, G., Constants of Diatomic Molecules, Van Nostrand Reinhold Company, 1979.

66. Torrens, I.M., Interatomic Potentials, Academic Press, 1972.

67. Bauer, E. and Poppa, H., "The Interaction of Oxygen with the Mo(100) Surface," Surface Science, v. 88, pp. 31-64, 1979.

INITIAL DISTRIBUTION LIST

		No. Copies
1.	Defense Technical Information Center Cameron Station Alexandria, Virginia 22304-6145	2
2.	Superintendent Attn: Library, Code 0142 Naval Postgraduate School Monterey, California 93943-5002	2
3.	Department Chairman, Code 61Sq Department of Physics Naval Postgraduate School Monterey, California 93943-5000	2
4.	Dr. Don E. Harrison, Jr. Code 61Hx Department of Physics Naval Postgraduate School Monterey, California 93943-5000	5
5.	Captain Philip J. Mattson, USA 906 Park Avenue Manteca, California 95336	6
6.	Lieutenant Dana Majors, USN 1064 Halsey Drive Monterey, California 93940	1

221101

Thesis
M38345 Mattson
c.1 Sputtering of chemisorbed nitrogen from the (100) planes of tungsten and molybdenum a comparison of computer simulation and experimental results.